2020

Development of a SOX9 Reporter Cell for High-Throughput Chondrogenic Assessment

Alyssa R. Mickle
University of Central Florida

DEVELOPMENT OF A SOX9 REPORTER CELL FOR HIGH-THROUGHPUT CHONDROGENIC ASSESSMENT

by

ALYSSA MICKLE

A thesis submitted in partial fulfillment of the requirements
for Honors in the Major Program in Biomedical Sciences
in the College of Medicine
and in the Burnett Honors College
at the University of Central Florida
Orlando, Florida

Fall Term, 2020

Thesis Chairs: Thomas Kean, PhD, and William Self, PhD

ABSTRACT

Osteoarthritis (OA) is a debilitating disease caused by the deterioration of articular cartilage and is a leading cause of disability in the United States and worldwide. Much current research into improved treatment for this disease is focused on tissue engineering through the growth of cartilage sheets made by articular chondrocytes. However, as chondrocytes proliferate *in vitro*, they also lose their ability to produce dense extracellular matrix, a necessary component of articular cartilage conferring mechanical strength. SOX9, a transcriptional activator, increases type II collagen expression, a key articular cartilage extracellular matrix component. Thus, SOX9 promotes an articular cartilage phenotype. Therefore, increasing SOX9 expression and activity as a transcriptional activator in culture has the potential to improve tissue engineering outcomes. This project serves to generate SOX9 promotor-driven secreted luciferase reporter chondrocytes to monitor chondrogenic properties temporally and non-destructively for use in high-throughput analysis of culturing conditions and drug screening.

DEDICATIONS

For Mrs. Rodriguez, who first showed me the wonders of science and inspired me to pursue it. Your work as an educator has touched not only my life but that of many others, and I promise it does not go unnoticed. For my partners-in-crime Katie Moskal and Brendon Cavainolo – we made it! For my family, and particularly my parents Nancy and Garrett Mickle, who have always been my number one supporters. I owe it all to you.

ACKNOWLEDGMENTS

I would like to thank my thesis chairs, Dr. Kean and Dr. Self who have been such incredible supporters. Dr. Kean, thank you for your fantastic mentorship, and for welcoming me to your new lab group; this has been the highlight of my college career. Dr. Self, from day one of my start at UCF you have been there to help guide me towards success. I cannot express how lucky I have been to have you both as such awesome advisors in my corner. Thank you also to Dr. Kyle Rohde for donating your time, support, and expertise as part of my committee. Additionally, thank you to the Caplan Lab at Case Western Reserve University for sharing the SOX9-gLuc plasmid.

TABLE OF CONTENTS

LIST OF FIGURES

LIST OF TABLES

CHAPTER ONE: INTRODUCTION

Osteoarthritis

Osteoarthritis (OA) is a chronic joint condition in which the articular cartilage covering the end of bones deteriorates, causing changes in cartilage composition and reduction in structural integrity. The response to this deterioration is inflammation, resulting in swelling, pain, and motion impairment. OA can be a product of joint overuse causing gradual degradation and usually develops with age, particularly in those who are overweight or have jobs that are demanding on the joints. It can also develop in younger people after traumatic, sudden injury. Both these sudden and overuse injuries cause lesions in the articular cartilage, which become progressively larger until the bone is completely exposed. Late stage OA is a serious disability, with extreme pain and loss of joint function [1]. Globally, around 303 million people are affected, and OA accounts for more than 10% of US national healthcare costs [2, 3].

Current treatments for OA

Treatment for osteoarthritis varies as the disease progresses, and often include prescription and over-the-counter painkillers, physical therapy or acupuncture, assistive devices such as canes or walkers, and eventually surgery such as total knee arthroscopy [4]. Further damage can sometimes be mitigated with gait training, weight management and other risk factor reduction. The most commonly recommended treatment is a course of non-steroidal anti-inflammatory drugs; however, patients only had moderate benefit from this plan [5]. As the disease progresses and pain can no longer be managed by other treatment plans, the last treatment option becomes surgery, such as a

total knee arthroplasty (TKA). TKA involves the removal of damaged tissue from the joint and the insertion of artificial materials at the bone interface. While this option usually results in reduced pain and increased function, one in five patients remain unsatisfied after the surgery. This may be due in part to complications arising after surgery which can include infections and periprosthetic failure or loosening. Additionally, the inserted prosthetics only last 15 to 20 years, making TKA a poor option for younger patients [6].

In 2005, osteoarthritis and other rheumatic diseases were the largest cause of reported disability in the US, making up 19% of the total [7]. An estimated 26.9 million Americans had symptomatic OA in 2008, increased from 21 million in 1995 [8]. The associated costs of OA for both medical expenses and lost income for those affected are also significant. For the average person diagnosed with OA at age 54, the direct medical costs of their condition total over $19,000 during their lives [9]. Additionally, people with OA lose $4,835 in income every year as a direct cost of their condition, resulting in a total attributable cost of $154.8 billion dollars per year in the US alone [10]. With the aging US population, OA disease instances and the associated costs will only increase in the coming years, making advancements in treatment options particularly impactful.

Tissue Engineering of Cartilage

Cell-Based Treatment Options

One cell-based technique for cartilage regeneration which has seen promise is autologous chondrocyte implantation (ACI). In this treatment method, samples of a patient's cartilage tissue

are removed from an area of the joint that is low load-bearing. These samples are then expanded in culture and re-implanted at the site of the cartilage defect [11]. A second-generation method, matrix-assisted autologous chondrocyte implantation (MACI), involves culturing the harvested cells on a collagen scaffold before implantation which improves cell distribution [12]. Short-term clinical outcomes for ACI are mostly positive, with one 3 year follow up study showing 84% of patients had improvements in pain and function while only 6% had graft failure [13].

Sadly, despite some success with ACI, the treatment still faces several difficulties. First, while ACI can be useful for treating small defects that may later lead to symptomatic OA, patients with OA often have defects much too large for this treatment to be effective [14]. Additionally, ACI requires that there be an undamaged area of the joint from which to harvest tissue, a requirement people with severe OA may not reach; even if such an area exists, the removal of tissue results in the production of an additional lesion [15]. Once grafted, the new tissues do not always integrate with the surrounding cartilage, leading to a weak graft that will ultimately fail [16]. After implantation, ACI grafts often do not produce hyaline cartilage, but fibrocartilage which has much worse mechanical properties [17]. Finally, as the tissue is re-implanted into a joint with significant damage and inflammation, it can be a challenge to ensure the grafted tissue remains healthy over time [14]. All of these limitations lead to poor long-term results; in a 10 year follow up study of patients who had undergone autologous implantation, 25% had one or more of their grafts fail [18].

Current State of Tissue Engineering in OA

The transcription factor SOX9 is a necessary factor in the differentiation of chondrocytes. Articular chondrocytes arise from mesenchymal stromal cells (MSCs), otherwise known as chondroprogenitors. These cells can ultimately differentiate into myoblasts, adipocytes, or osteoblasts, as well as chondrocytes. For an MSC to differentiate into a chondrocyte, it must express SOX9, a transcription factor which promotes expression of proteins necessary for chondrogenesis including type II collagen and aggrecan [19]. SOX9 is expressed in cells undergoing mesenchymal condensation, and people with mutated SOX9 have severe skeletal deformations, indicating that SOX9 is necessary for appropriate chondrocytic and skeletal development [20]. Additionally, studies of mice chimeras have shown that cells lacking SOX9 do not contribute to the formation of cartilage [21]. SOX9 was also shown to be necessary for chondrogenesis from mouse embryonic fibroblasts, as when expression is silenced through siRNA, bone morphogenetic protein-2 (BMP-2) was unable to stimulate differentiation [22].

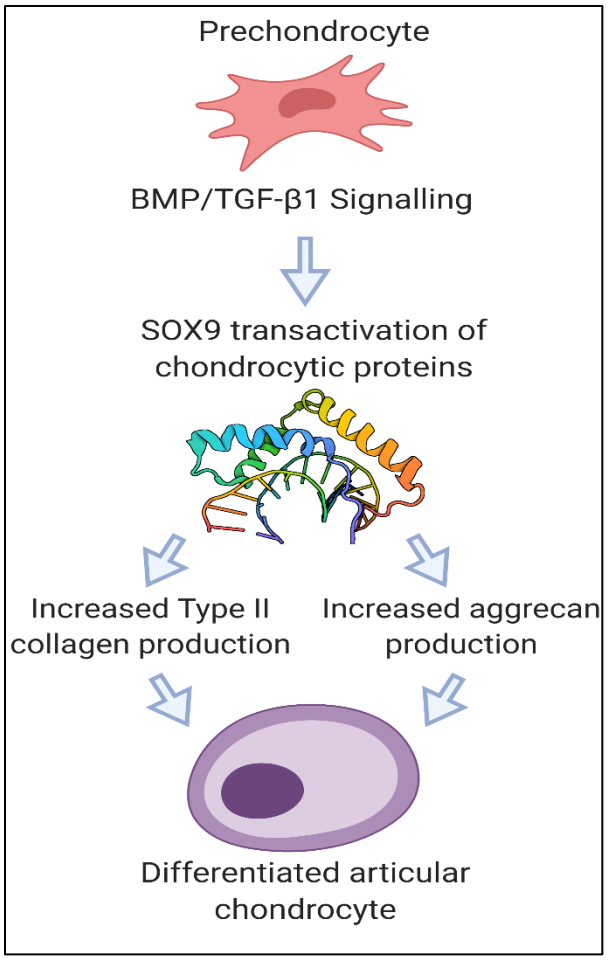

Figure 1: SOX9 in Chondrogenic Differentiation
SOX9 activates the transcription of proteins essential to articular cartilage extracellular matrix such as aggrecan and type II collagen. Differentiation to a chondrocytic line does not occur without this factor. Created with BioRender.com.

Current culture methods for cartilage tissue face several problems, the largest of which is the de-differentiation of cells resulting in a reduction of SOX9 and type II collagen production that occurs with prolonged monolayer culture. Monolayer culturing of cells is necessary to increase the number of cells in order to have enough to form new tissue. While freshly harvested chondrocytes initially express high levels of type II collagen and proteoglycans, after serial culture in monolayer

the cells stop having this phenotype and switch from their usual cuboidal morphology to a fibroblastic elongated and flatter morphology [23]. A 2003 study of human articular chondrocytes (HACs) found that after of 21 days in culture and in subsequent serial cultures, the levels of type II collagen, a protein necessary for articular cartilage which is activated by transcription factor SOX9, dropped dramatically, down to 100-fold less by day 28. Type II collagen is a major component of the extracellular matrix that dictates the mechanical strength of cartilage and its loss is therefore an indicator of de-differentiation in culture [24]. Further studies have shown that in culture, these cells also lose their ability to produce chondromodulin and glycosaminoglycans. Proliferation of HACs on tissue culture plastic causes de-differentiation [25]. Immortalized cells can show distinct phenotypic differences to primary cells and are a poor representation of the *in vivo* environment. Being able to track the expression of SOX9 non-destructively will allow us to optimize culture methods to keep chondrocytes in a chondrogenic state.

With the shortcomings of using ACI to repair only small defects, new cell-based tissue engineering treatment options to resurface the entire joint are being explored. Tissue engineering refers to the production of a biological rather than inorganic material to replace or restore tissues or even whole organs [17]. However, like traditional ACI, tissue engineering must surmount the problem of the de-differentiation of cells in culture. Research into effective tissue engineering of articular cartilage includes questions about cell source, scaffolding, signal molecules for growth induction, and mechanical stimulation methods. The cell type chosen must be accessible and numerous while still maintaining chondrocytic properties, and the environmental factors must encourage production of SOX9, type II collagen, and other chondrocytic marker proteins to combat de-differentiation. All of these factors must be adjusted and optimized for production of a large

quantity of cells with appropriate chondrogenic properties to make an engineered cartilage that is an effective replacement for damaged tissues [26]. To do this, these factors must be adjusted by quantifying how they affect the mechanical and molecular properties of the cell.

Destructive Methods of Tissue Visualization

Genetic, biochemical, and mechanical quantification methods have been used to help determine what conditions are best for the growth of cartilage in culture. The effect of variables such as scaffolds [27], oxygen tension [28], and growth on extracellular matrix [29] among others on the properties of cultured chondrocytes have all been tested and used to improve culture methods. These variables' effects are commonly determined using terminal destructive assays on the tissues to quantify factors like the type II collagen and glycosaminoglycan (GAG) content, or mechanical properties like shear and aggregate modulus, or the tissue's deformation under load. GAG location can be determined through staining and histological evaluation, while its amount can be quantified through biochemical assays. The expression of proteins like type II collagen can be determined by ELISA, while gene expression can be determined by evaluating the mRNA content of the cell [29]. Mechanical properties of cartilage tissue are commonly evaluated by subjecting a punch sample of a cartilage sheet to an indentation test [27].

While the terminal, destructive methods listed above provide useful information about a tissue's properties, they have several drawbacks. Firstly, terminal methods only provide information about the result and whatever times are chosen to be sampled rather than continuous temporal information. This prevents one from making time related insights, which can be critical as properties may change dramatically as the cells proliferate and differentiate. Additionally, destructive methods require that some portion of the tissue must be used exclusively for testing.

This is a problem when using these assaying methods to determine sample quality, as these properties may vary widely from sample to sample. Finally, these methods are time consuming and do not easily allow for high-throughput screening of many culture conditions at once [30]. Therefore, there is a need to develop non-destructive methods that are easy to quantify and can be used to track changes in properties temporally to advance cartilage cell culture techniques for tissue engineering.

SOX9 as an Indicator for Cartilage Success

Overview of Cartilage and Chondrocytes

Cartilage develops as an embryonic tissue that is the basis for adult skeletal elements. Much embryonic cartilage ultimately calcifies into bone, but some cartilage remains into adulthood, including that of the trachea, nose, ear, and articular cartilage in the joints. Articular cartilage is of particular interest as it is subjected to stresses in the joint and is therefore prone to morbidities such as osteoarthritis [31]. Articular cartilage is an avascular tissue made up of chondrocytes, a specialized cell type, and the extra-cellular matrix (ECM) those cells produced structured in several layers. These layers provide protection from varying stresses; the outer layer, called the tangential zone, is a very thin layer that protects from shear stresses. Beneath this layer is the transitional zone, which provides some resistance to compressive forces, and the deep zone that provides the most compressive resistance. These zones differ in the organization and composition of the extracellular matrix, giving them their unique properties. Finally, a layer of calcified ECM and hypertrophic chondrocytes provides an anchorage between cartilage and the bone [32].

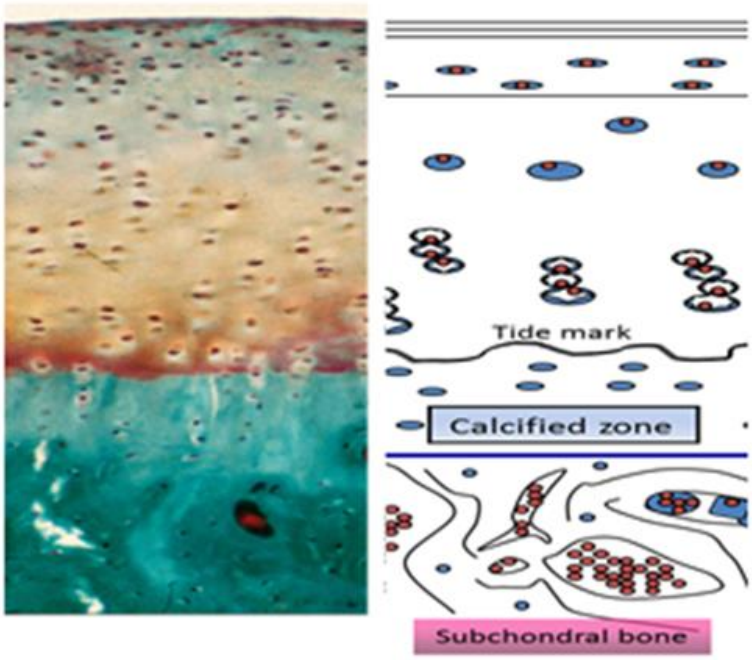

Figure 2: Articular Cartilage Composition
The histology section on the left shows a safranin-O stained piece of articular cartilage. Red stain indicates presence of GAG. The green stain clearly shows the tidemark where cartilage becomes calcified and becomes subchondral bone. The cartoon on the right shows the different areas of the tissue. At the top, chondrocytes are more flattened, becoming rounded as you go deeper into the tissue before becoming columnar in structure. (Figure adapted from J.E. Dennis, unpublished)

The one cell type in cartilage, the chondrocyte, functions to build and maintain the ECM which gives cartilage its mechanical properties. These cells are extremely sparse in adult cartilage, making up only 2% of the volume of cartilage tissue. As cartilage is avascular, the cells rely on diffusion and metabolize primarily anaerobically. The dense ECM produced by the chondrocytes prevents cell movement throughout the tissue, contributing to the inability of cartilage tissue to successfully repair itself once damaged [32]. While there is little cell-to-cell signaling of chondrocytes due to their isolated nature, these cells can respond to mechanical stimuli as well as growth factors and cytokines by remodeling the ECM surrounding them. A chondrocyte's ECM

is made up predominantly of collagens and proteoglycans; type II collagen is the predominant collagen while aggrecan is the predominant proteoglycan [32].

There are several cell lines often used as an approximation of human articular chondrocytes for various research purposes, including mouse embryonic fibroblasts [22] and rat chondrosarcoma cells [33]. One such cell line, ATDC5 cells, are sourced from teratocarcinoma fibroblasts from mice. These cells closely follow the differentiation pathway of human articular chondrocytes, and express the chondrocytic phenotype of type II collagen and aggrecan [34]. Additionally, they respond to transcription factors such as SOX9. ATDC5s also proliferate quickly, and expand in an undifferentiated form; these benefits, along with their close approximation of human articular chondrocytes, make them a good model for chondrocytic research [35].

Role of SOX9 in Differentiation

Bone morphogenetic proteins (BMPs), specifically BMP-2, have been shown to induce chondrogenesis in ATDC5 cells, promoting early differentiation as well as the increase in type X collagen seen in late differentiation to hypertrophy [36]. BMP-2 signaling activates two pathways: BMP-2/Smad, and BMP-2/p38, both of which alter SOX9 activities, levels, or both. The Smad pathway only affects SOX9 activity but does not alter mRNA content, while the p38 pathway affects both SOX9 activity and expression. BMP-2 stimulates transcription of SOX9 by increasing binding of the transcription activator NF-Y to the CCAAT region on the gene's promotor [22]. Once BMP-2 increases SOX9 expression and activity, the SOX9 protein acts as a transcriptional activator of a number of genes encoding proteins necessary for chondrogenesis. These genes fall

under several categories, most notably genes encoding ECM proteins and those that regulate the ECM such as modifying enzymes, transporters, or receptors [37].

SOX9 levels are high during early differentiation and decrease as chondrocytes move towards hypertrophy, making temporal quantification of SOX9 particularly important. As SOX9 begins to commit MSCs to a chondrocytic line, the cells first begin to condense. Cells that ultimately form the articular cartilage will begin producing dense ECM. Meanwhile, those of the growth plate proliferate and drop out of the cell cycle, differentiating into pre-hypertrophic chondrocytes which then increase in volume by almost 20 times, converting to hypertrophic chondrocytes. Eventually these hypertrophic chondrocytes calcify the ECM surrounding them, which osteoclasts degrade for osteoblasts to turn into bone matrix. Hypertrophic chondrocytes stop expressing SOX9 and begin expressing type X collagen rather than type II, as well as other hypertrophic markers like RUNX2. These terminally differentiated chondrocytes then die, or as some recent evidence suggests, may go on to further re-differentiate into osteoblasts [38]. Chondrocytes in the articular cartilage begin to undergo hypertrophy during OA disease progression [39], losing the phenotypic expression of type II collagen needed for healthy cartilaginous ECM. As type II collagen provides articular cartilage with its resistance to shear and tensile stress [32], SOX9 levels act not only as an indicator of the differentiation state of chondrocytes, but also as an indirect measure of their mechanical properties.

Additionally, SOX9 levels in OA are downregulated as compared to typical cartilage tissue [20], making the transcriptional activator a potential target for OA drugs, a treatment option which is currently lacking. Developing drugs is a costly process, with high rates of failure. The overall approval rate for a development program is only 13.8% [40] with an average cost to develop of

$985 million [41]. A good cellular model that appropriately mimics the *in vivo* environment can help prevent expensive attrition at later clinical trial stages, reducing costs and speeding up the development process. Given SOX9's importance to the phenotype of chondrocytes, having a fast, simple, and non-destructive method of quantifying its expression could lead to great improvements in osteoarthritis treatment.

Non-Destructive Luciferase-Based Reporting

Luciferases, proteins which emit light in the presence of luciferins, are widely used. Their luminescence can be used for imaging or to quantify cellular properties by linking luminescence levels to a characteristic of interest such as promotor activity. *Gaussia* luciferase (Gluc) is a secreted luciferase; this means its levels can be quantified directly from media, making it very convenient for measuring cells in culture, particularly 3D spheroids [42]. Lentiviruses are pathogens which insert their genetic material into their hosts genome. While they cause a variety of serious diseases such as HIV, their ability to transport RNA from outside a cell into the nucleus and incorporate it into the existing genetic material makes them a useful tool in gene editing. Lentiviral vectors are based on HIV but separate the genes for infectivity and transfer of viral DNA onto different plasmids. This ensures that the vector can infect only a single cell and cannot propagate and spread, making it a safe method of gene transduction [43]. Using lentiviral transduction and Gluc, SOX9 levels can be quantified non-destructively by transducing cells with the gene for Gluc under the control of the SOX9 promotor. Under conditions in which the SOX9 promotor is activated, Gluc is produced, allowing promotor activation to be easily quantified by luminescence assays.

Several studies have successfully transduced SOX9 into various chondrocytic cell lines, and some work has been completed with non-destructive reporters [20, 30, 44]. While it was still ultimately a destructive assay, transduction of SOX9 tagged with green fluorescent protein and FLAG tags into human articular chondrocytes to increase those cell's production of SOX9 was used to determine what genes SOX9 regulates [20]. In this case, the genes regulated were determined using an RNA hybridization microarray analysis [20]. Their expression levels were quantified with quantitative real time PCR, simply comparing expression levels in native tissue to tissue with SOX9 upregulated by its additional transduction into the cell [20]. A secreted luciferase reporter system for promotors of SOX9, aggrecan, and osteocalcin has also been transduced into bone marrow derived human mesenchymal stem cells (hBM-MSCs) to determine the effect of certain conditions on the differentiation of MSCs into chondrocytes [30]. As these probes do not require destruction of samples for quantification, they are well suited to studying the temporal changes that accompany differentiation [30]. The use of secreted luciferase reporters to assess the effect of culture conditions on chondrogenic properties has also been met with success. A luciferase reporter driven by type II collagen promoter was transduced into ATDC5 cells to determine optimal culture media components needed for improved production of type II collagen [44]. The use of this reporter allowed for high-throughput testing of a wide variety of media components in varying quantities [44]. These previous successes bode well for similar success with transducing a SOX9 promotor luciferase reporter into ATDC5's and human articular chondrocytes for high-throughput screening applications.

With the widespread and increasing impacts of osteoarthritis, the need for improvements in OA care and treatments is vital. Current treatments have some success but are all subject to

drawbacks including limitations in efficacy, scale, or longevity. Much work is being done in tissue engineering to grow enough cartilage tissue to resurface entire joints. However, this technology has several hurdles to surmount before it is a viable treatment, including that chondrocytes tend to de-differentiate as they are expanded in culture. Determining conditions for cell culture to support growth of chondrocytes that produce high quality ECM requires that the protein composition and mechanical properties of the experimental tissues be readily measurable. Historic measurement techniques give only a snapshot of current properties and require sample destruction, making them inadequate for the high-throughput methods necessary to quickly drive the field forward. The use of promotor-driven luciferase reporter cells to quantify the expression of certain key proteins in chondrocyte development has shown success for several applications already, allowing for temporal evaluation without sample destruction. As SOX9 is instrumental in the differentiation of chondrocytes, the development of a SOX9 reporter cell allows for improved testing of the effect of various culturing conditions on the molecular signature of chondrocytes. Additionally, as SOX9 levels are reduced in osteoarthritis, transducing such a promotor into human articular chondrocytes creates a cellular system that could act as a high-throughput screen for osteoarthritis drug development.

CHAPTER TWO: PRODUCTION OF REPORTER CELLS

Materials and Methods

Preparation of Plasmid

Use of lentiviral-based vectors for genetic editing has been made safer by separation of viral replication genes into several plasmids, including the packaging plasmid psPAX2 (Plasmid #12260; Addgene), envelope gene plasmid pMD2G (Plasmid #12259; Addgene), and transgene plasmid, in this instance SOX9-gLuc (Fig 3; 9,405 bp, Genecopoeia). To generate the necessary quantity of plasmid for lentiviral production, competent *E. coli* (GCI-L3; Genecopoeia) were transformed with each of the three vectors individually. These *E. coli* were grown in LB media containing glycerol and ampicillin (0.4%), lysed, and the plasmid purified out using a commercial maxiprep kit (ZymoPURE^{TM} II Plasmid Maxiprep Kit; Zymo Research Corp). Plasmid purification and concentration was determined using a spectrophotometer (NanoDrop, ThermoFisher Scientific). Finally, confirmation of the plasmid was verified by running gel electrophoresis (0.7% w/v agarose in TBE) on both purified plasmid and plasmid linearized by restriction enzyme digest using BamH1 compared to a gene fragment ladder of known lengths (FastDigest BamH1 ThermoFisher Scientific).

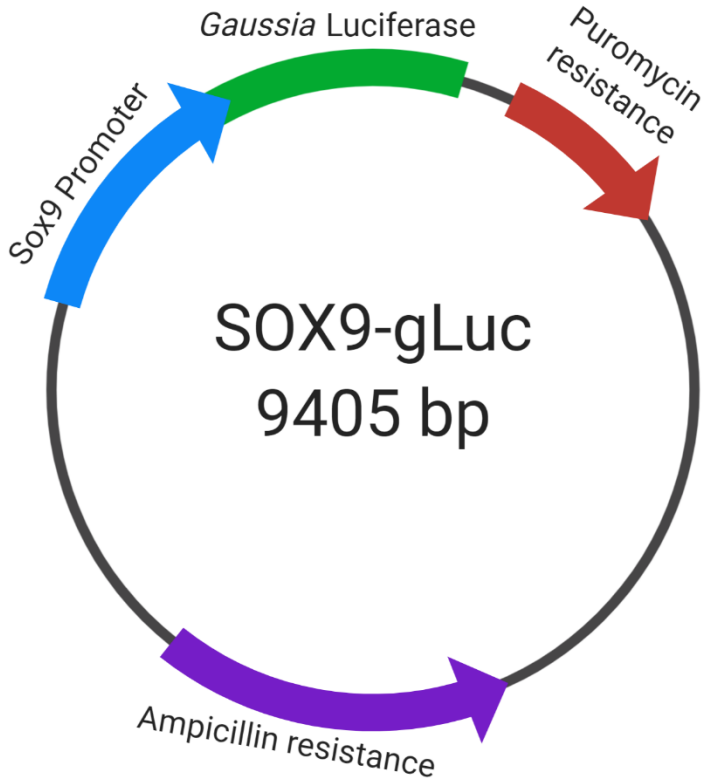

Figure 3: Plasmid Map for SOX9-gLuc
The plasmid contains Gaussia luciferase under the control of the SOX9 promoter. Additionally, it contains a gene for ampicillin resistance to select for transformed E. coli, as well as a gene for puromycin resistance to select for transduced chondrocytes. Created with BioRender.com.

Lentivirus Generation

To generate the lentiviral particles for transduction, HEK293Ta cells were transfected with the 3 plasmids already grown and purified: pMD2G, psPAX2, and SOX9-gLuc, using calcium phosphate nanoparticles. Plasmids were combined in equimolar concentrations in HEPES buffered saline, then precipitated out while vortexing in calcium solution [45]. These nanoparticles were added to the cells and incubated overnight (37 ºC, 5% CO_2). Media was then replaced the next day

(after ~12 hours) with HEK293Ta growth media. The conditioned growth media containing the lentiviral particles was collected daily over 72 hours, and the lentiviral particles were concentrated through ultracentrifugation (15,000 RCF on a 10% sucrose gradient) [46]. Particles were serially diluted from 1x to 0.0001x concentrations.

Cell Culture and Infection

After the lentiviral particles were generated, concentrated, and serially diluted, they were added to ATDC5 cells in a 24-well plate (Corning Costar) in the presence of polybrene (4 µg/ml, EMD Millipore) to enhance infection. These cells were grown for two passages in puromycin to select for those that were transduced. Additionally, non-infected ATDC5 cells were grown in both standard and puromycin containing growth media (DMEM low glucose with 5% FBS and 1% pen/strep) to act as positive and negative controls. An initial evaluation of luminescence from media of all the cell lines determined which cells were significantly infected to establish the cell line to use in further applications. To evaluate luminescence, 50 µl of coelenterazine substrate mix [47] (BioLux® Gaussia Luciferase Assay Kit; New England BioLabs) were added to 20 µl media samples from cells exposed to each concentration of virus as well as non-infected ATDC5s by an OT-2 pipetting robot (Opentrons OT-2). Luminescence was recorded in relative light units by a 96 well plate reader (EnVision) at 25º C, and luminescence of each cell line was compared to the non-infected control.

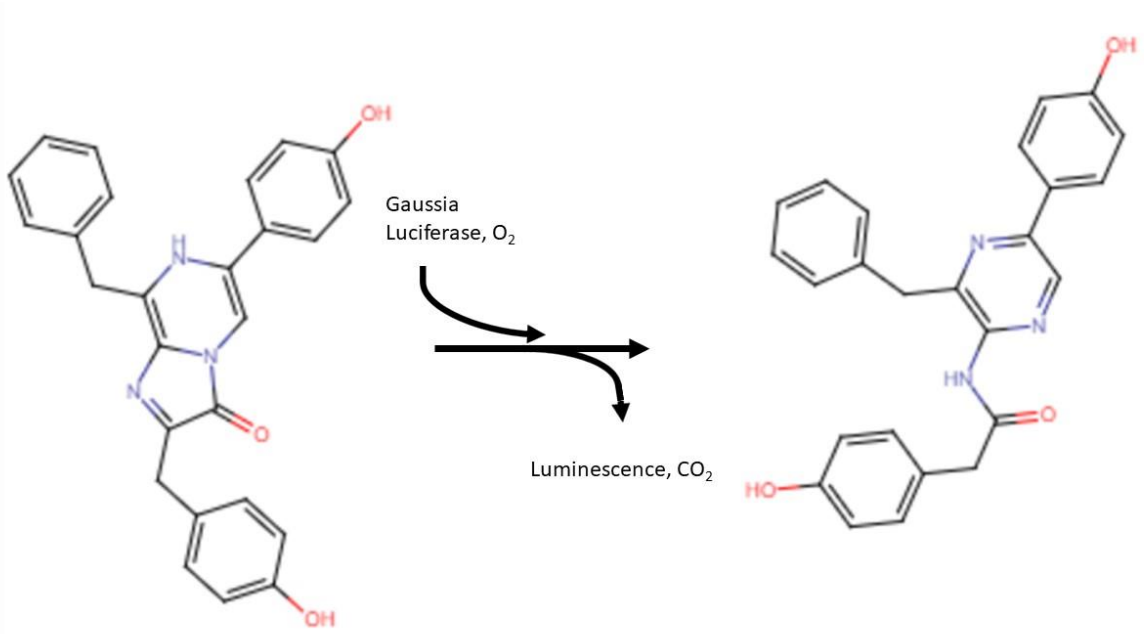

Figure 4: Gaussia Luciferase's Catalysis of Coelenterazine to Coelenteramide

Titration of Lentivirus

Evaluation of lentiviral concentration was determined by extraction of viral RNA from concentrated media, cDNA synthesis using a commercial kit, and qRT-PCR on the purified RNA product compared to standards (Lenti-Pac HIV qRT-PCR Titration Kit, GeneCopoeia). The activity of particles generated was determined through a functional titer by serially diluting them before infecting ATDC5s. mRNA was extracted from ATDC5-gLuc cells using a commercial kit (PureLink RNA Mini Kit, Invitrogen), mRNA purity and concentration were evaluated using RNA ScreenTape (Agilent), and cDNA was synthesized normalized to mRNA concentration. qRT-PCR was run on RNA isolated from the cells to establish the effectiveness of infectivity, with primers designed to amplify murine SOX9, gLuc, and the reference genes HPRT and PPIA (Table 1).

Table 1: Primers for qRT-PCR

	Forward Primer	Reverse Primer
mSOX9	5'-GAGGAAGTCGGTGAAGAACGGA-3'	5'- GTTTTGGGAGTGGTGGGTGG-3'
gLuc	5'-ACGCTGCCACACCTACGA-3'	5'-CCTTGAACCCAGGAATCTCAGGAA-3'
mHPRT	5'-AAGTTTGTTGTTGGATATGCCC-3'	5'-CTCATCTTAGGCTTTGTATTTGGC-3'
mPPIA	5'- GGTCCTGGCATCTTGTCCAT-3'	5'- GCCTTCTTTCACCTTCCCAAA-3'

Results and Discussion

Plasmid Purity and Concentration

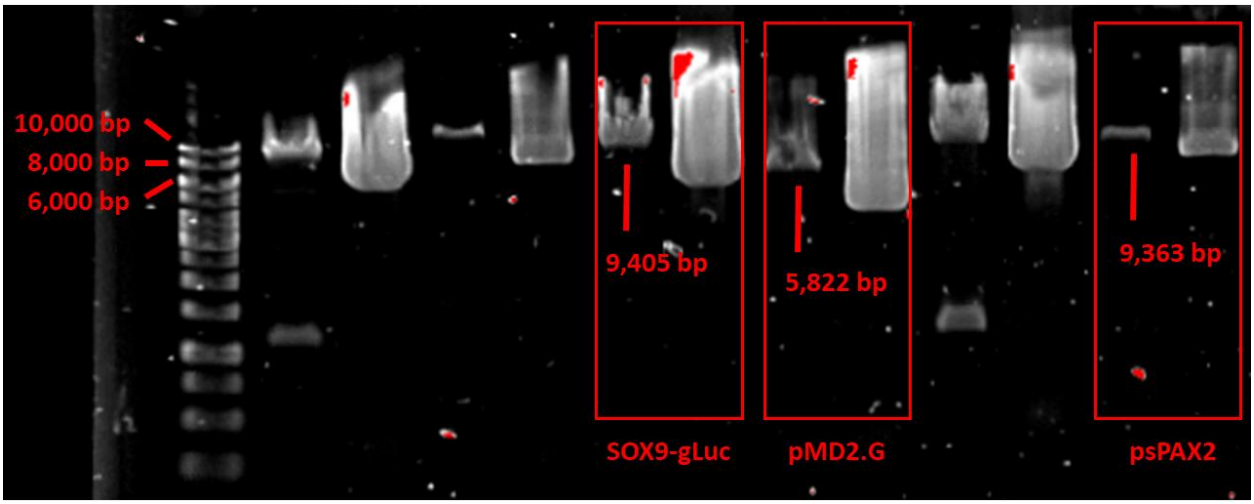

Figure 5: Plasmid Digested by BAMH1 and Run on 0.7% Agarose Gel
From left to right: 1 kb gene ruler (Thermo Fisher Scientific), Col10A1-gLuc digested and undigested, OC-fLuc digested and undigested, SOX9-gLuc digested and undigested, pMD2.G digested and undigested, RunX2-gLuc digested and undigested, psPAX2 digested and undigested.

Nanodrop spectroscopy showed that the purification produced plasmid at a sufficient concentration and quantity for lentivirus production. As shown in Figure 5, digestion and gel electrophoresis of the plasmid gave bands that confirm the plasmid's identity and showed it to be sufficiently pure.

Initial Luminescence Evaluation

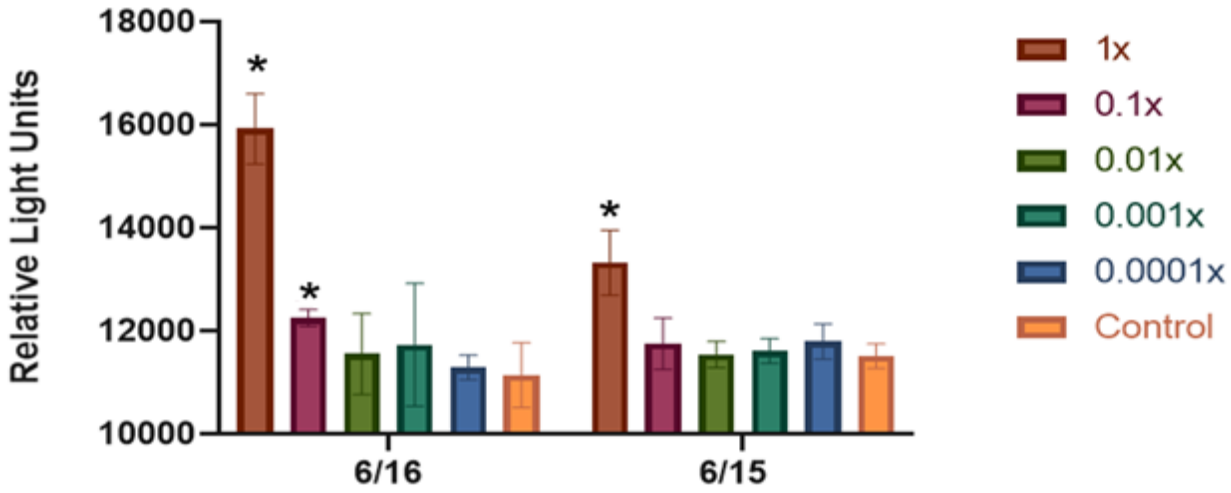

Figure 6: Luminescence Assay on Media from Newly Infected Cells
* indicates $p < 0.05$. Cell lines with significant luminescence were 6/16 1x, 0.1x and 6/15 1x.

Of the ATDC5-gLuc cell lines infected with serially diluted lentivirus, only the 1x and 0.1x of virus generated on 6/16 and the 1x of virus generated on 6/15 had luminescence that was significantly greater than the non-infected ATDC5s. No upper concentration of virus resulted in cell death, indicating that viral titers were likely low.

Lentiviral Titers

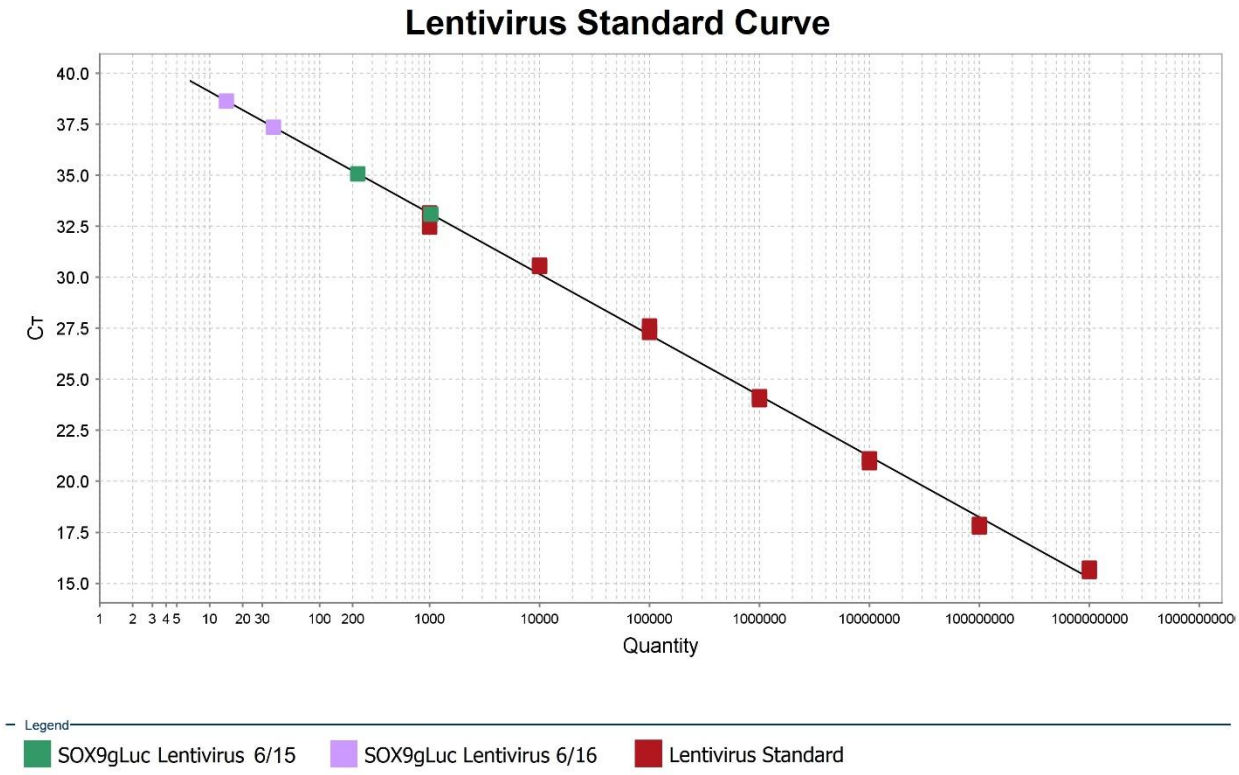

Figure 7: Standard Curve for qRT-PCR Based Lentivirus Titer
Quantification of viral copy number per milliliter.

The lentivirus qRT-PCR titer confirmed low titers, with neither lentivirus produced on 6/16 or 6/15 falling within the range of lentivirus standards. Lentivirus standards fit the curve well, with an R^2 of 0.96. The 6/16 virus had an average value of 42,188 particles/ml, while 6/15 had an average value of 945,313 particles/ml. While the qRT-PCR titer for the 6/15 standards was higher than that produced on 6/16, as they were both outside of the standard range this was inconclusive. Additionally, the absolute number of viral particles does not necessarily indicate the number that are infectious. This requires a functional titer e.g. with ATDC5 cells.

For the functional cell infection titer, normalized to reference genes and compared to the ATDC5-gLuc sample of 6/15 1 x, the 6/15 1 x had a relative quantification (RQ) of 1.0 and the 6/16 1 x had a RQ of 0.797. The 6/16 0.1 x cells did not cross the threshold within 40 cycles. While qRT-PCR titers showed a higher production of lentivirus on 6/15, the functional cell infection titers indicated that 6/15 and 6/16 1 x had much closer levels of infection than expected. Therefore, since the initial quantification of luminescence was much higher for 6/16 1 x cells and there was not a significant difference in functional titers, the 6/16 1 x cells were chosen to be used in further applications.

CHAPTER THREE: DOSE RESPONSE TO TGF-β1

Materials and Methods

Production of High-Density Pellets

As they performed best in the initial evaluation of luminescence, cells from the 6/16 1x lentiviral cell line (ATDC5-gLuc) and non-infected ATDC5 cells were trypsinized, resuspended in basal chondrogenic media (Dulbecco's modified Eagle's medium high glucose supplemented with pen/strep, dexamethasone, ITS + premix, glutamax, pyruvate, MEM non-essential amino acids, ascorbate-2-phosphate, and fungizone [29, 44]), counted via hemocytometer, and seeded in a 96-well non-adherent u-bottom plate (Greiner) at a cell density of 50,000 cells per well in 200 µl media. Only the inner wells were seeded with cells, while the outer wells were filled with PBS to ensure a consistent environment with limited media evaporation. Six rows containing six pellets each of both ATDC5-gLuc and non-infected ATDC5s were seeded across two plates. The plates were centrifuged (500 x g, 5 minutes) to initiate pellet formation and were then incubated at physiological oxygen tension (37 ºC, 5% CO_2, 5% O_2) to allow for pellet contraction. This was considered day 0. Transforming growth factor beta 1, or TGF-β1, is known to induce chondrogenesis and should therefore increase SOX9 promotor expression. Six different dilutions of TGF-β1 (10, 1, 0.5, 0.1, 0.05, and 0.01 ng/mL) in chondrogenic media were used to establish a dose-response curve between TGF-β1 and the luminescence values from luciferase assays on the growth media. The day after pellet formation, the basal chondrogenic media was replaced with media containing TGF-β1. This first feeding and sampling was considered day 1.

Cell Feeding and Sampling

Cells were fed and sampled every Monday, Wednesday, and Friday through day 21. 150 µl of old media were removed, 20 µl of which were placed in a white 96 well plate (Greiner Bio-One) for luminescence evaluation, as described in Chapter 2. 150 µl of new media was added back to each of the wells, and bright-field images of each pellet was taken with an ImageXpress Pico system (Molecular Devices). Pellet size was analyzed from the microscope images using ImageJ, first by applying a binary mask and then measuring total area, circularity, and solidity for each area larger than 1000 pixels. Luminescence of ATDC5-gLuc cells compared to non-infected ATDC5s for each condition and day was evaluated using multiple t-tests.

Pellet Harvesting

After sampling and imaging on day 21, pellets were harvested for end-of-experiment RNA analysis and histology. Five pellets were removed from media and placed in 300 µl of RNA lysis buffer (Purelink RNA Mini Kit, Invitrogen) containing β-mercapatoethanol. The pellets were homogenized, and the RNA was purified with a commercial kit using on-column DNase (PureLink RNA Mini Kit, Invitrogen). mRNA purity and concentration were evaluated using RNA ScreenTape (Agilent), and cDNA was synthesized for qRT-PCR evaluation. qRT-PCR (2x SYBR Green PCR mix, ThermoFisher Scientific) was run on each sample amplifying mSOX9 and gLuc and the reference genes mPPIA and mHPRT as described in Chapter 2. Each experimental condition was a single biological replicate of five pellets with two technical replicates. The final pellet was removed from media and placed in 300 µl of neutral buffered formalin for histology, and then transferred into PBS after 24 hours. Pellets were placed into square mesh cassettes and processed for 30 minutes in 70% ethanol, 60 minutes in 95% ethanol , 30 minutes 100% ethanol,

80 minutes in xylene, and paraffin for an hour (Leica ASP300S). Processed tissue was embedded in paraffin wax (Leica Biosystems Embedder) and left overnight at 4°C to harden before sectioning. Blocks were sectioned at 5 µm thick (Leica Biosystems RM2125 RTS), and sections were floated in a water bath at 50°C before being fixed to slides (VWR Superfrost) which were baked overnight at 40°C. Slides were deparaffinated and then stained with hematoxylin, Fast Green FCF, and Safranin-O. Coverslips were attached above the stained pellet sections with a resin mounting media (Cytoseal) which was allowed to dry overnight before imaging with an ImageXpress Pico system (Molecular Devices).

Results and Discussion

Luminescence Assays

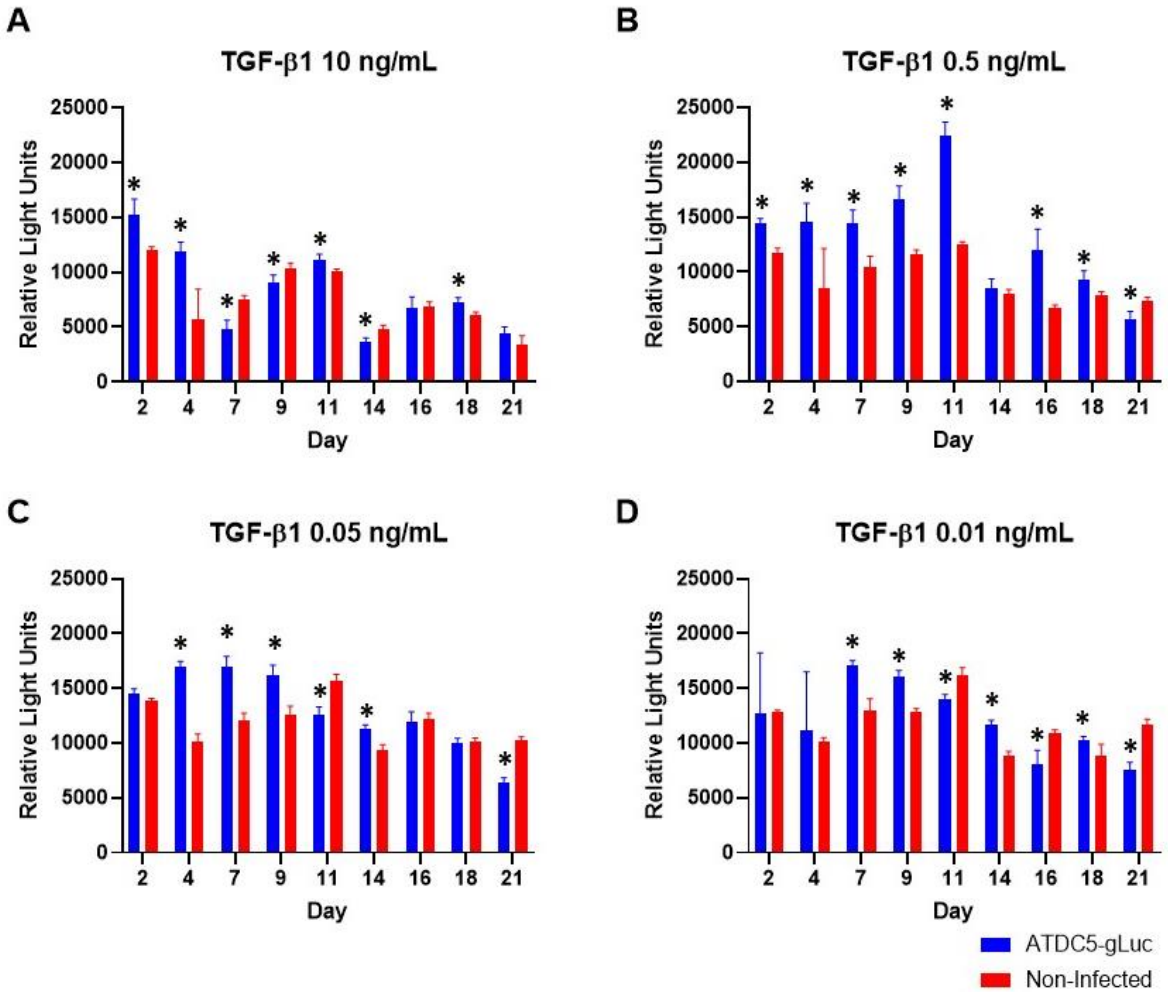

Figure 8: Luminescence of ATDC5-gLuc cells treated with TGF-β1 over 21 days
Relative light values of ATDC5-gLuc and non-infected cells. * indicates $p < 0.05$ for multiple t-tests of ATDC5-gLuc and non-infected.
A: 10 ng/mL TGF-β1. B: 0.5 ng/mL TGF-β1. C: 0.1 ng/mL TGF-β1. D: 0.01 ng/mL TGF-β1.

The highest concentration,10 ng/ml TGF-β1 as shown in Figure 8A, was expected to have the strongest signal, since TGF-β1 induces chondrogenesis. While the first two timepoints had significant luminescence, beyond that the luminescence unexpectedly dropped off. This may be

due to an increase in metabolism causing a drop in pH below luciferase's optimal range, which was suggested by a difference in well color after the addition of substrate compared to samples containing less TGF-β1. The kit used for evaluation of luminescence uses a buffered solution, and so increasing the buffering capacity may improve luminescence readings for samples with high metabolic activity. This is especially possible for days where the ATDC5-gLuc cells had a luminescence significantly lower than background, such as days 7, 9, and 14. As shown for the 0.5 and 0.01 ng/ml TGF-β1 (Figures 8 B and C), significant luminescence was seen as late as day 18, indicating that the signal was not transient, and that lower concentrations of TGF-β1 may shift the time period of chondrogenesis later. This shift in chondrogenesis with TGF-β1 dosage illustrates the potential for having non-destructive evaluation methods such as this for temporal analysis. However, with poor initial viral titers, the signal to background ratio is very low. Along with an improvement of the assay buffer, an additional round of lentiviral particle generation and improved infection of the reporter cell line will be necessary to increase luminescence of the reporter line.

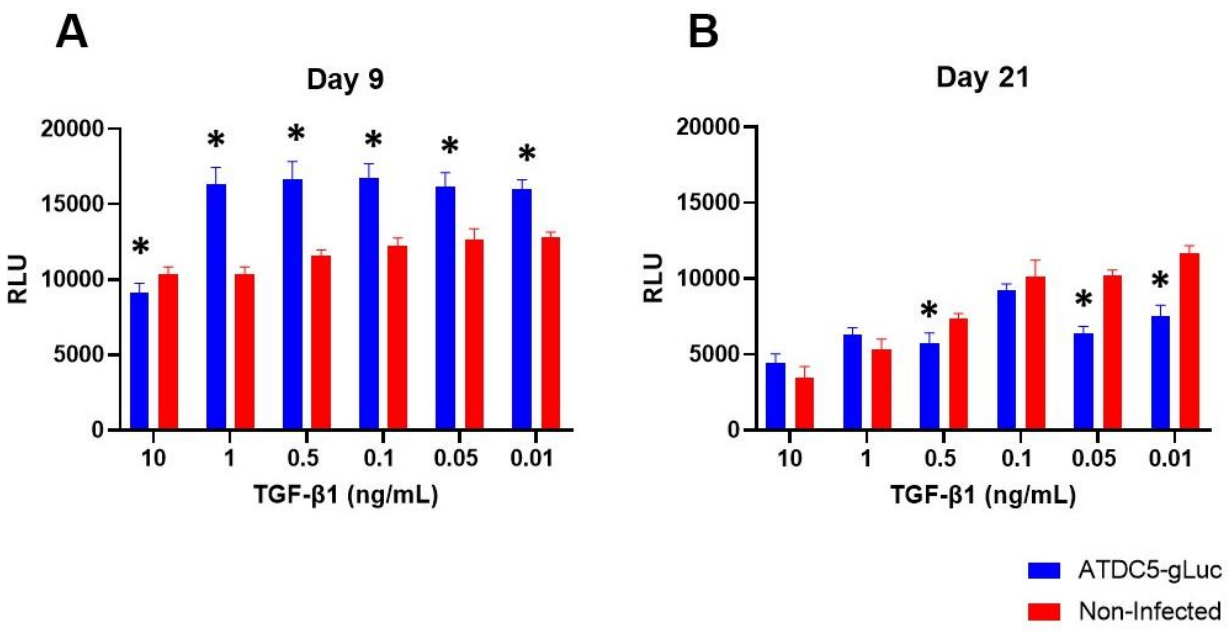

Figure 9: Luminescence of ATDC5-gLuc Cells on Day 9 and 21
Relative light values of ATDC5-gLuc and non-infected cells. * indicates $p < 0.05$ for multiple t-tests of ATDC5-gLuc and non-infected.
A: Day 9. B: Day 21

Day 9 (Figure 9A) had high luminescence of ATDC5-gLuc above non-infected ATDC5s for all conditions but 10 ng/mL which had already dropped off by day 7. However, by day 21 (Figure 9B), luminescence for ATDC5-gLuc was not significantly higher for any conditions and was in fact lower than non-infected for 0.5, 0.05, and 0.01 ng/mL. This may indicate that the pellets were reaching hypertrophy, as SOX9 levels decrease at this point. Further study could explore this possibility through qRT-PCR evaluation of hypertrophic markers such as osteocalcin.

Unfortunately, the time intervals between each sampling were not constant. This may have caused the inconsistency in background luminescence of non-infected cells. This lack of background consistency across days, combined with how luminescence is measured in relative light units which is specific to the plate reader rather than an absolute value, means that it is

difficult to compare luminescence between days on the same pellet. Consistency may be improved enough to allow for time point comparison by sampling at regular intervals.

Pellet Size Evaluation

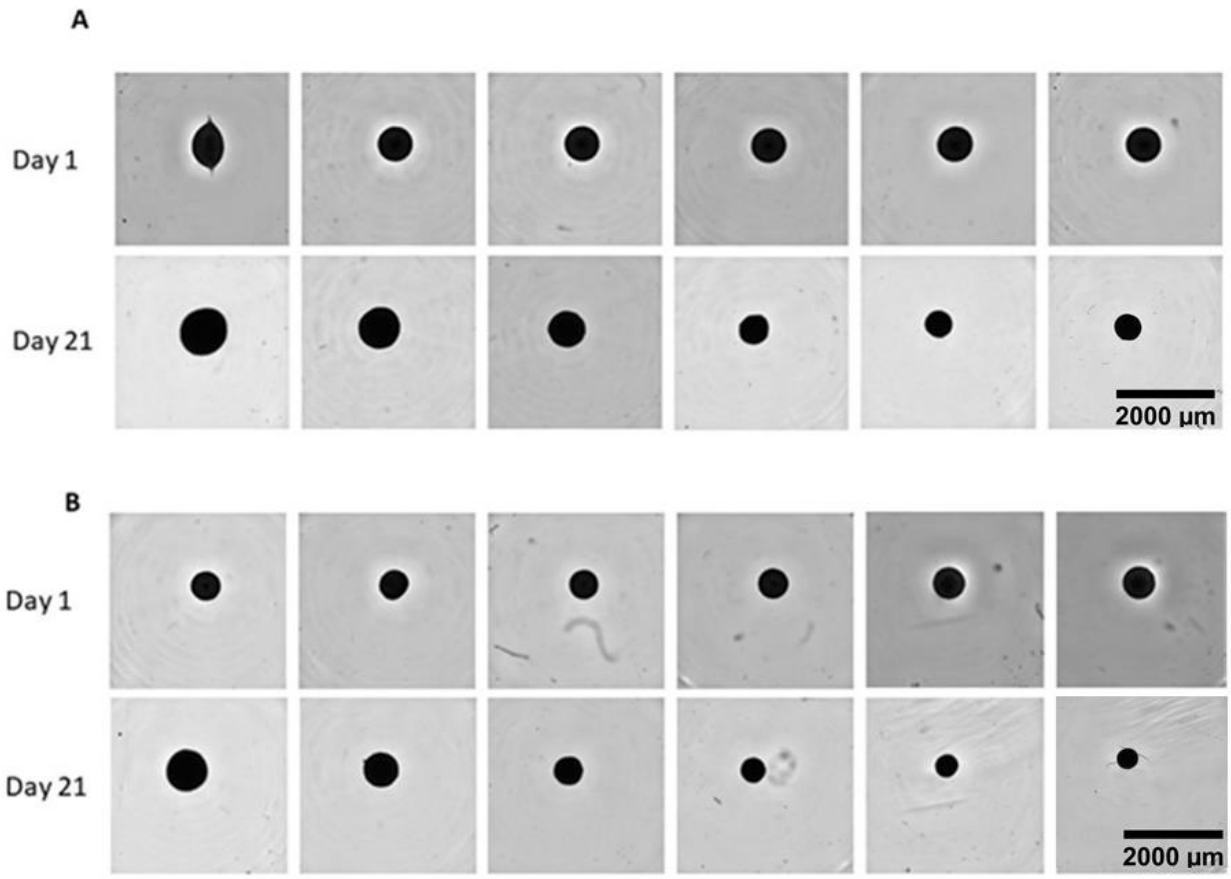

Figure 10: TGF-β1 Pellet Images, Days 1 and 21
A: ATDC5-gLuc cells B: Non-infected ATDC5s
From left to right, 10 ng/ml, 1 ng/ml, 0.5 ng/ml, 0.1 ng/ml, 0.05 ng/ml, 0.01 ng/ml TGF-β1. Scale same for each photo.

Both the ATDC5-gLuc and non-infected pellets started out with consistent sizing across TGF-β1 dosage, but by day 21 there was a very clear pellet size dose-response to TGF-β1 (Figs. 10, 11, 12). Pellet imaging indicated that infection did not alter the cells' growth, as both ATDC5-gLuc and non-infected cells reacted identically to the addition of TGF-β1.

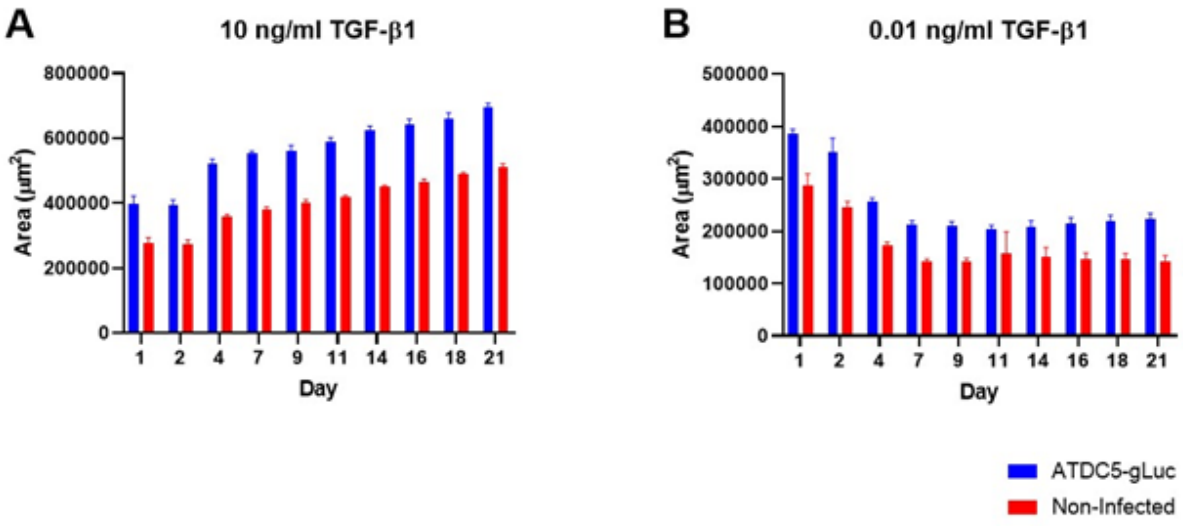

Figure 11: TGF-β1 Pellet Size
Area of ATDC5-gLuc and non-infected cells.
A: 10 ng/mL TGF-β1. B: 0.01 ng/mL TGF-β1.

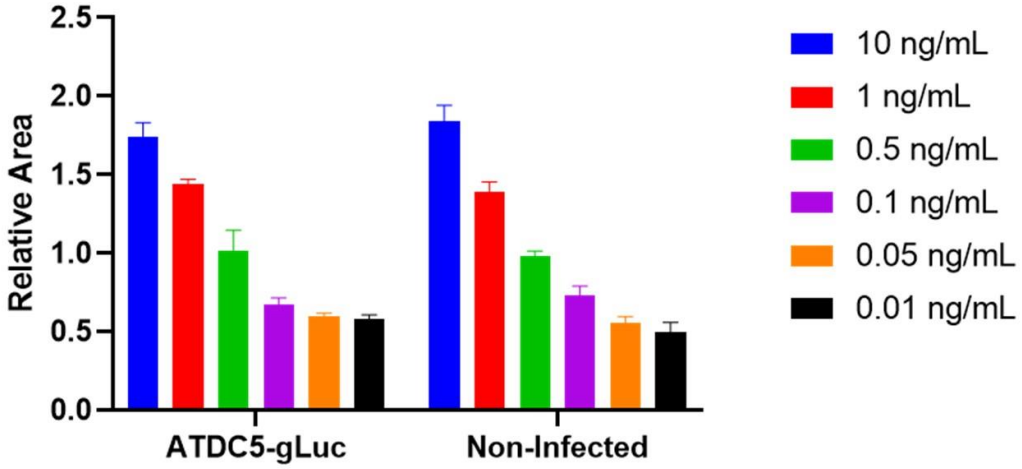

Figure 12: TGF-β1 Pellet Size on Day 21 Normalized to Day 1
Area of ATDC5-gLuc and non-infected cells normalized to the initial pellet size at day 1.

The ATDC5 non-infected pellets seem to have been seeded initially at a lower density than the pellets, but they changed in size proportionally to the higher density ATDC5-gLuc pellets over time, further supporting that infection does not change pellet morphology. The 10 ng/ml pellets (Figure 11A) increased in size over time; as these cells were undergoing chondrogenesis, cell replication is arrested and so an increase in size is likely due to production of extra cellular matrix. This contrasts with the 0.01 ng/ml pellets (Figure 11B) which decreased in size over the first week before stabilizing. The initial size decrease may be a continuation of the initial contraction seen in the first 24 hours of culture before they reach their most dense at the end of the first week. By day 21 (Figure 12), a dose-response of pellet size to TGF-β1 simulation was clear. As with the size change of the 10 ng/mL TGF-β1 over time, the differences of size with dose indicates increased production of ECM proteins with TGF-β1 dosage, and the identical response of ATDC5-gLuc to non-infected cells provides further evidence that infection did not significantly interfere with cellular growth.

qRT-PCR Analysis

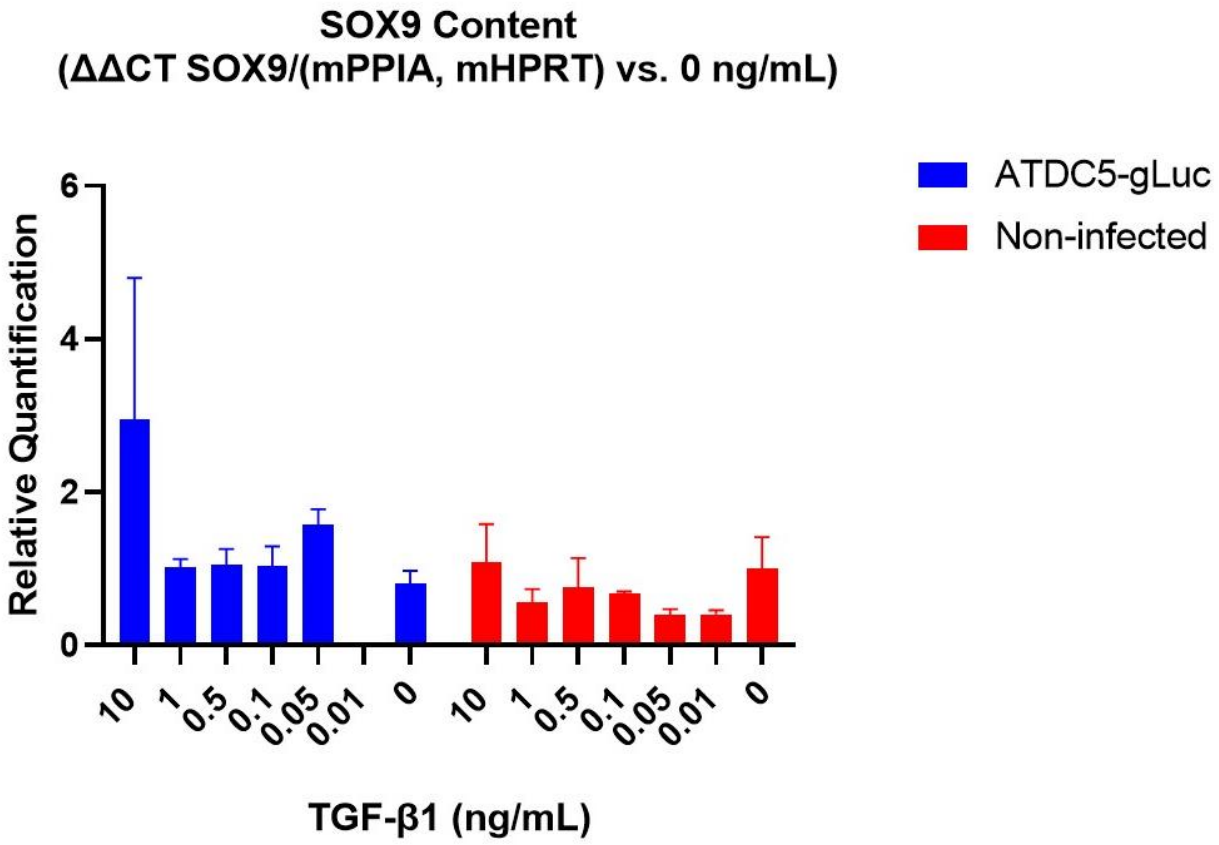

Figure 13: SOX9 Expression with TGF-β1 Dose
Relative Quantification of SOX9 content compared to 0 ng/mL.

qRT-PCR showed a lack of SOX9 response to TGF-β1 dosage at harvest on day 21 (Figure 13), supporting the lack of dose-response in luminescence on day 21. While there were large variances in relative quantification between samples, there was no significant difference in expression between ATDC5-gLuc and non-infected cells.

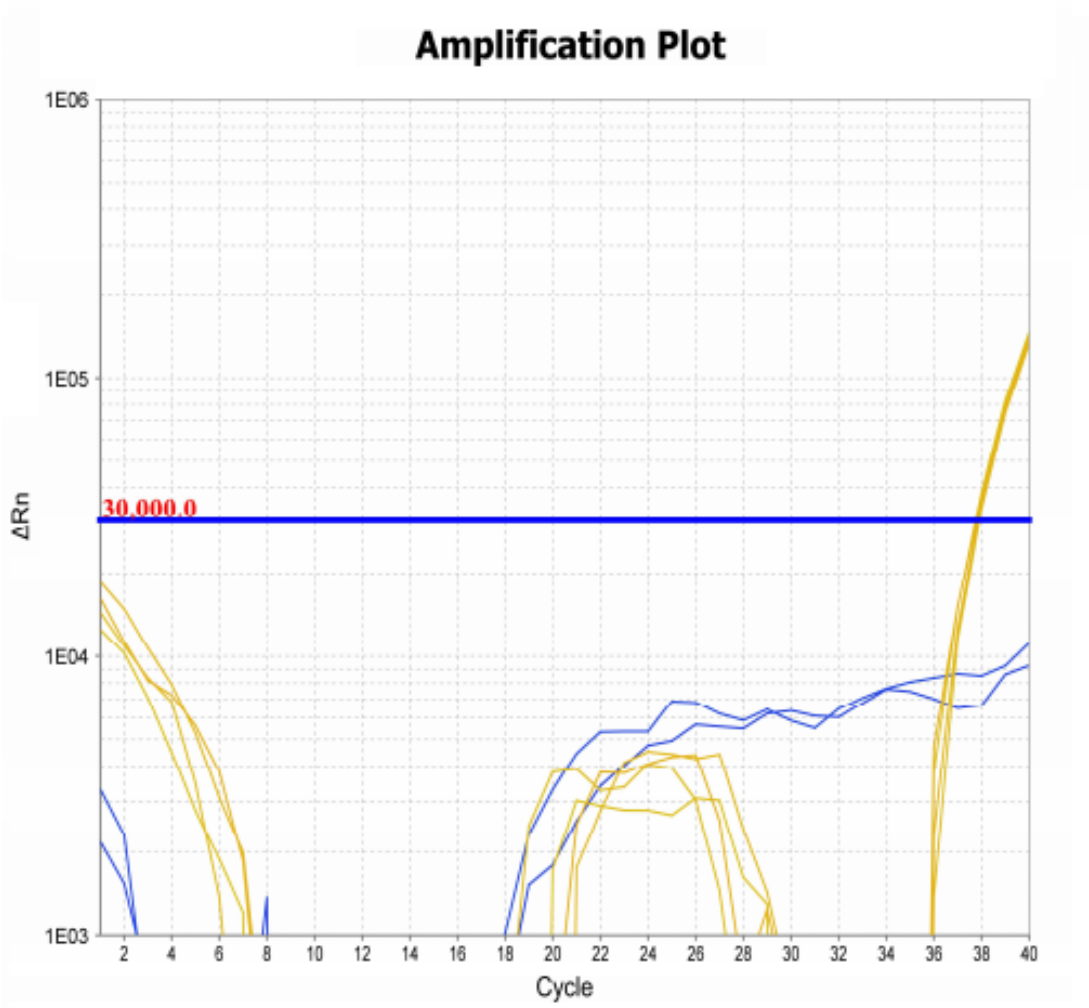

Figure 14: gLuc Amplification Plot for ATDC5-gLuc and Non-infected Cells
Yellow amplification plot lines for ATDC5-gLuc samples, while blue amplification plot lines for non-infected cells.

Only ATDC5-gLuc cells showed expression of gLuc, further supporting infection and that signal was not transient (Figure 14). At harvest of pellets, the gLuc expression did not follow TGF-β1 doseage, nor did it correlate well to luminescence at day 21. Additionally, gLuc expression did not correlate with SOX9 expression for the ATDC5-gLuc cells (Figure 15). However, as with the SOX9 expression, variance for gLuc relative quantification was quite high and so small differences between samples may be obscured by this. As mRNA extraction from cells grown in condensed

pellets is difficult and results in lower yeilds and purity than extraction from monolayer cells, lysing of more than five pellets may be necessary to generate sufficient mRNA yeild to reduce the variance. With this lack of correlation between the two, further work to establish the correlation will include reinfection of reporter cells with higher titer lentivirus to generate reporter cells with increased gLuc expression and higher signal to background. Additionally, cells will be grown in monolayer to facilitate mRNA extraction, and qRT-PCR will be completed at an earlier timepoint when SOX9 expression is still elevated.

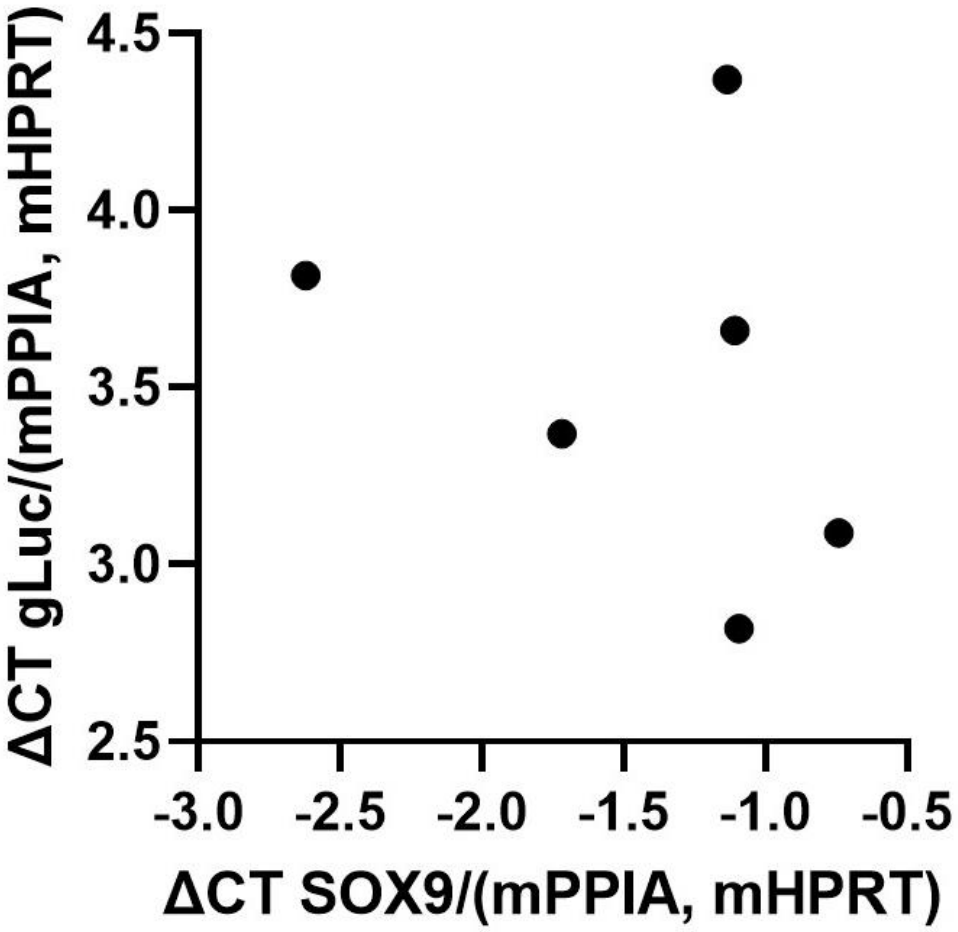

Figure 15: gLuc vs. SOX9 Expression
CT normalized to reference genes mPPIA and mHPRT

Histology

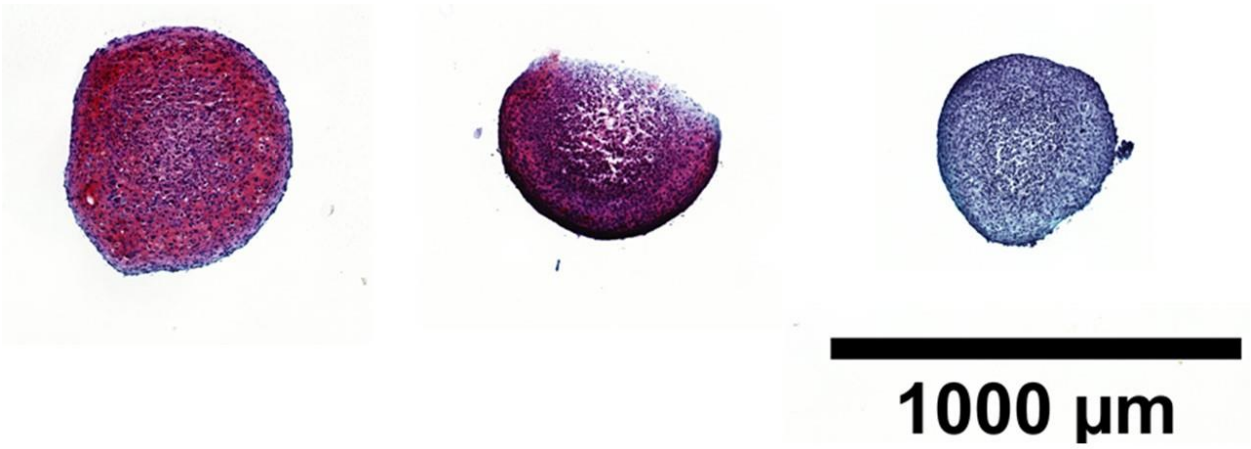

Figure 16: ATDC5-gLuc Histology for TGF-β1 Dose-Response
From left to right, 10 ng/ml, 1 ng/mL, and 0.5 ng/mL TGF-β1

Histological staining of pellets across the TGF-β1 dosage shows a change in proteoglycan content with dose (Figure 16). While the 10 and 1 ng/mL concentrations are similar in staining intensity, by 0.5 ng/mL there is a sharp drop off in proteoglycan content. This supports the usage of 1 ng/mL dosage in culturing media, as higher concentrations do not result in large increases in ECM protein production. It is expected that increasingly smaller dosages of TGF-β1 would have even less proteoglycans; however, these pellets had end sizes too small to effectively embed and section. Exploring the histological characteristics of pellets grown in these lower TGF-β1 concentrations would require seeding cells at a higher density upon pellet formation to generate larger pellets.

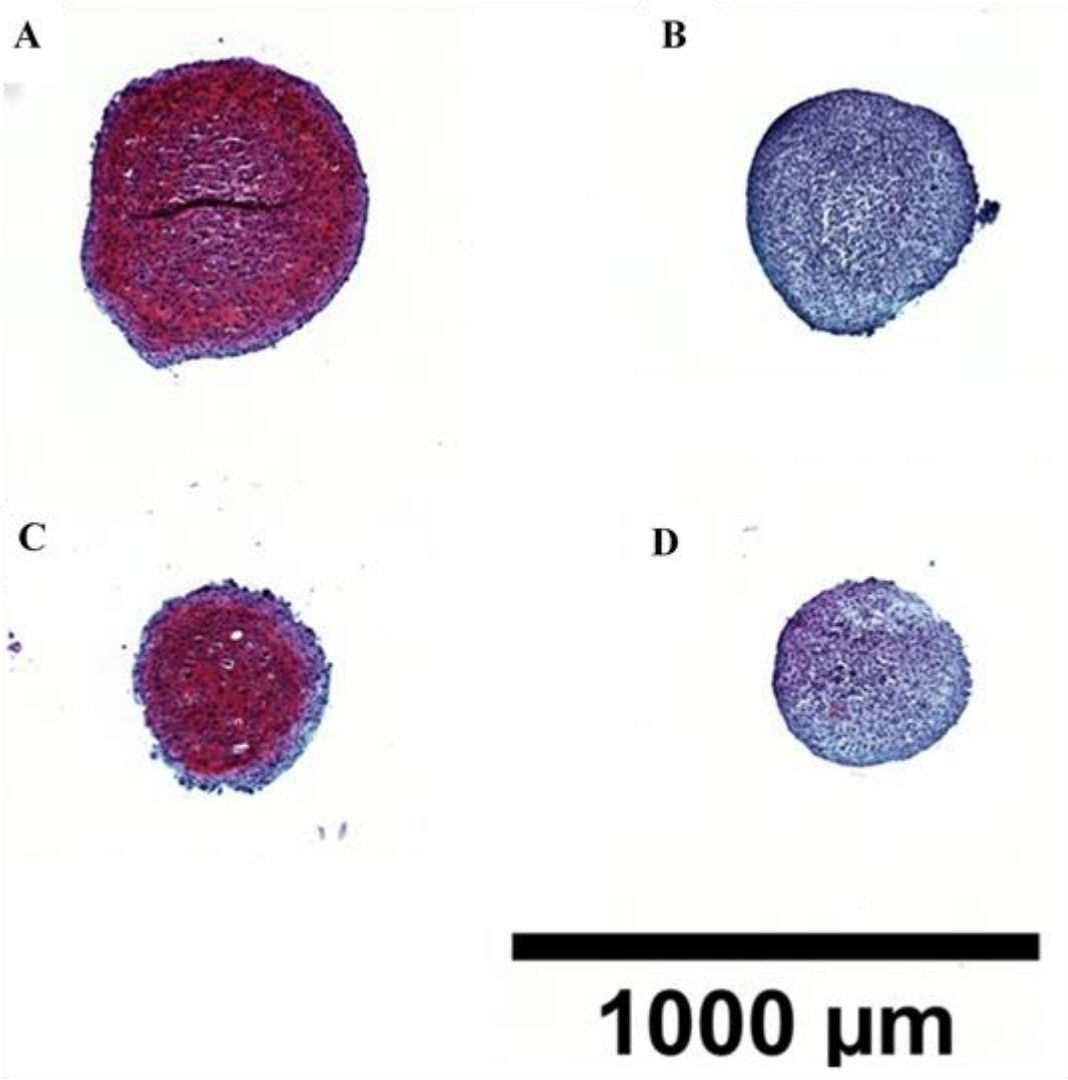

Figure 17: ATDC5-gLuc vs. Non-Infected Histology
A: 10 ng/mL ATDC5-gLuc B: 0.5 ng/mL ATDC5-gLuc C: 10 ng/mL Non-infected D: 0.5 ng/mL Non-infected

While differing in size, a comparison of ATDC5-gLuc and non-infected cells at both 10 and 0.5 ng/mL show comparable staining patterns (Figure 17). This identical response offers even more evidence that infection did not appreciably change cell growth characteristics.

CHAPTER FOUR: OPTIMIZED MEDIA COMPARISON

Materials and Methods

Media Generation

Traditional defined chondrogenic media (i.e. media lacking undefined components such as fetal bovine serum) used for chondrocyte differentiation is lacking in several vitamins and minerals known to be necessary in chondrogenesis. This Traditional media is Dulbecco's modified Eagle's medium high glucose supplemented with pen/strep, dexamethasone, ITS + premix, glutamax, pyruvate, MEM non-essential amino acids, ascorbate-2-phosphate, and fungizone. This lab has postulated an Optimized media with components at levels shown to increase type II collagen promoter driven mRNA production individually [44]. The Optimized media uses Traditional media as a base, with 15 added vitamins and minerals that are found in vivo (chromium 28 pg/ml, cobalt 90 fg/mL, copper 6.7 ng/mL, iodine 92 pg/mL, manganese 12 pg/mL, molybdenum 0.2 pg/mL, linolenic acid 27 ug/mL, retinoic acid 78 pg/mL, biotin 3 pg/mL, vitamin B12 914 pg/mL, vitamin D 8.6 fg/mL, vitamin K 11 ng/mL, zinc 120 pg/mL, and thyroxine 25 pg/mL). The vitamins and minerals were split into water soluble and ethanol soluble groups and a 2,000x stock of both groups was created. Optimized media was generated through addition of the 2,000x stocks to previously defined chondrogenic media while Traditional media was generated by adding equivalent volumes of ethanol and water as a control. Cells were split into two groups, receiving Traditional and Optimized media. Past studies have seeded pellets in traditional media on day 0 so that the first media change on day 1, post pellet contraction, is the point at which stimulation with vitamins and minerals occurs. To prevent aspiration of the pellet, only 75% of the media is replaced. Therefore, to stimulate the cells on day 1 and from seeding, Optimized and Traditional

media at 111% and 133% of the target vitamin and mineral concentration was generated to elucidate the effect of vitamin and mineral addition timing. Cells were split into two groups of those receiving vitamins on day 0 (D0) and those receiving vitamins on day 1 (D1).

Cell Seeding, Feeding, and Sampling

Cells from the 6/16 1x lentiviral cell line (ATDC5-SOX9gLuc), non-infected ATDC5 cells (ATDC5), and previously infected reporter cells for type II collagen (ATDC5-COL2gLuc) for use as a positive control in luciferase assessment were trypsinized, resuspended in traditional chondrogenic media, and counted via hemocytometer. The cells were diluted with additional traditional chondrogenic media to reach a cell density of 2.5 million cells/mL. 20 µl of cells (50,000 total) per well of each cell type were seeded into two columns of a 96-well non-adherent u-bottom plate (Greiner). Each column (6 pellets) received either 180 µl of 111% traditional or optimized media; these were considered D0 cells. An additional 2 columns of each cell type were seeded with 20 µl cell suspension and 180 µl of chondrogenic media; these were considered D1 cells. On the following day, D0 cells were fed with 1x traditional or optimized media, while D1 cells were fed with the 133% traditional or optimized medias to reach a final concentration of 100%. This was considered day 1, and cells were fed, imaged, and assayed for luciferase every Monday, Wednesday, and Friday for 21 days as described in Chapter 3. At each subsequent feeding, both D0 and D1 cells received 1x optimized or traditional media. At the end of 21 days, the pellets were harvested for histology and qRT-PCR also as described in Chapter 3.

Results and Discussion

Luminescence Assays

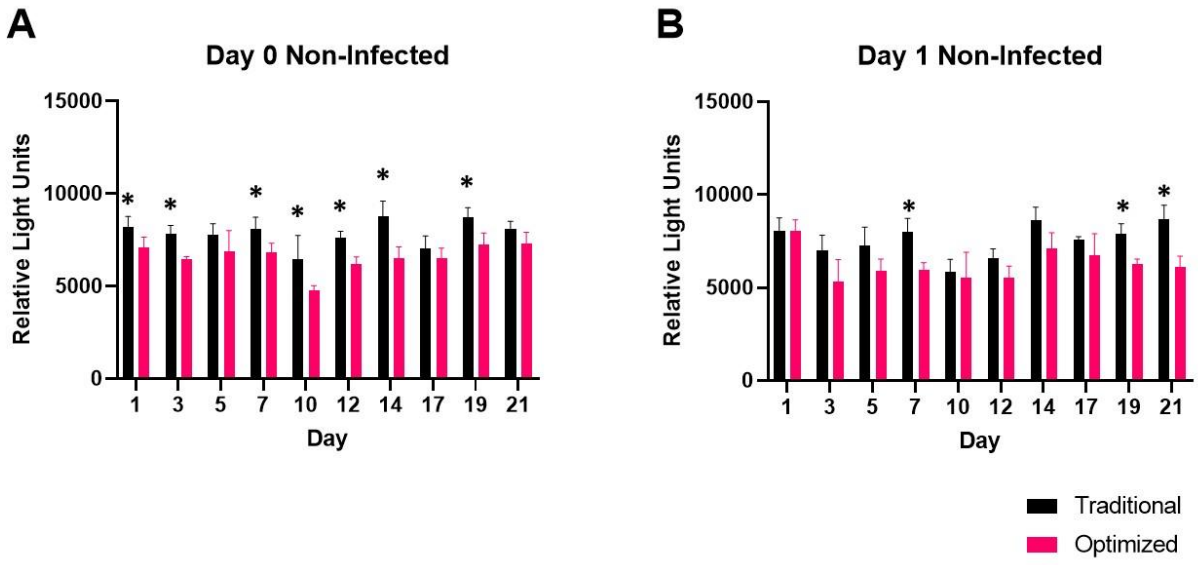

Figure 18: Luminescence of Non-Infected Cells Stimulated on Day 0 and 1
Relative light values of non-infected cells. * indicates $p < 0.05$ for multiple t-tests of traditional and optimized media.
A: Day 0. B: Day 1.

In this assay, for both Day 0 and Day 1 stimulated cells, luminescence levels for non-infected ATDC5s (Figure 18) were significantly higher for traditional media than for optimized media. This difference varied by up to 2000 RLUs on several days of the assay. Since these pellets were not infected, the difference is an intrinsic property of the media, indicating that one or more of the additives themselves lowered luminescence values. To account for this difference, luminescence for reporter cells was normalized to the background values for the non-infected ATDC5s in either traditional or optimized media.

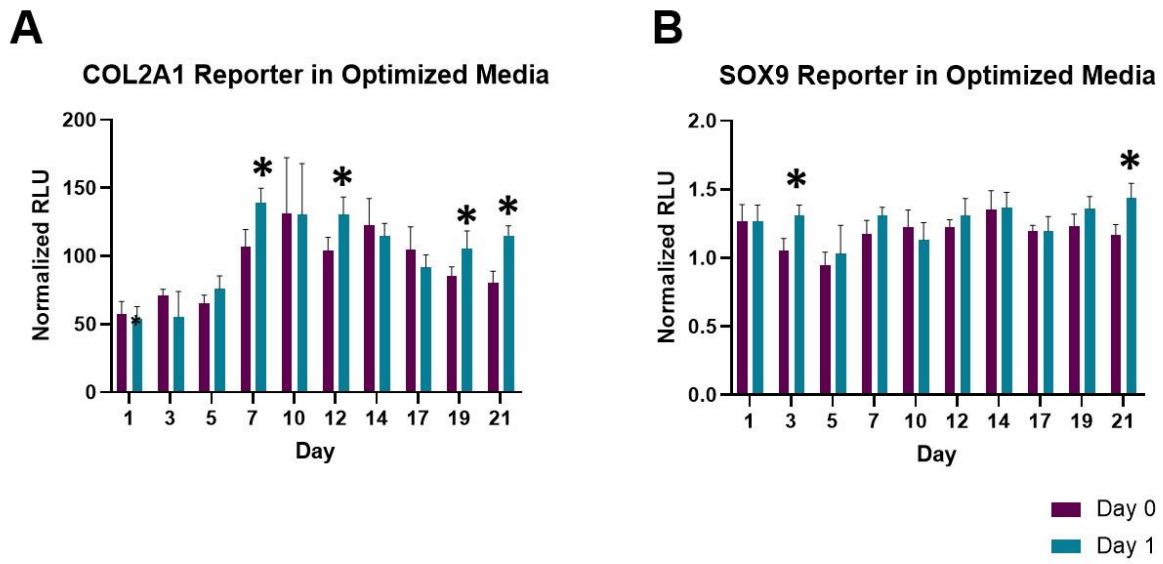

Figure 19: Luminescence of ATDC5-gLuc in Optimized Media Added on Day 0 and Day 1
Relative light values of ATDC5-gLuc cells normalized to non-infected. * indicates $p < 0.05$ for multiple t-tests of Day 0 and Day 1.
A: COL2A1 Reporter. B: SOX9 Reporter

For cells stimulated with vitamins, luminescence was significantly higher on some days for day 1 addition than day 0 addition. Interestingly, despite 1x media being added to both conditions every day past day one, the days with a significant difference in luminescence for day 1 stimulated cells occurred later on, with day 21 significantly higher for both SOX9 and type II collagen.

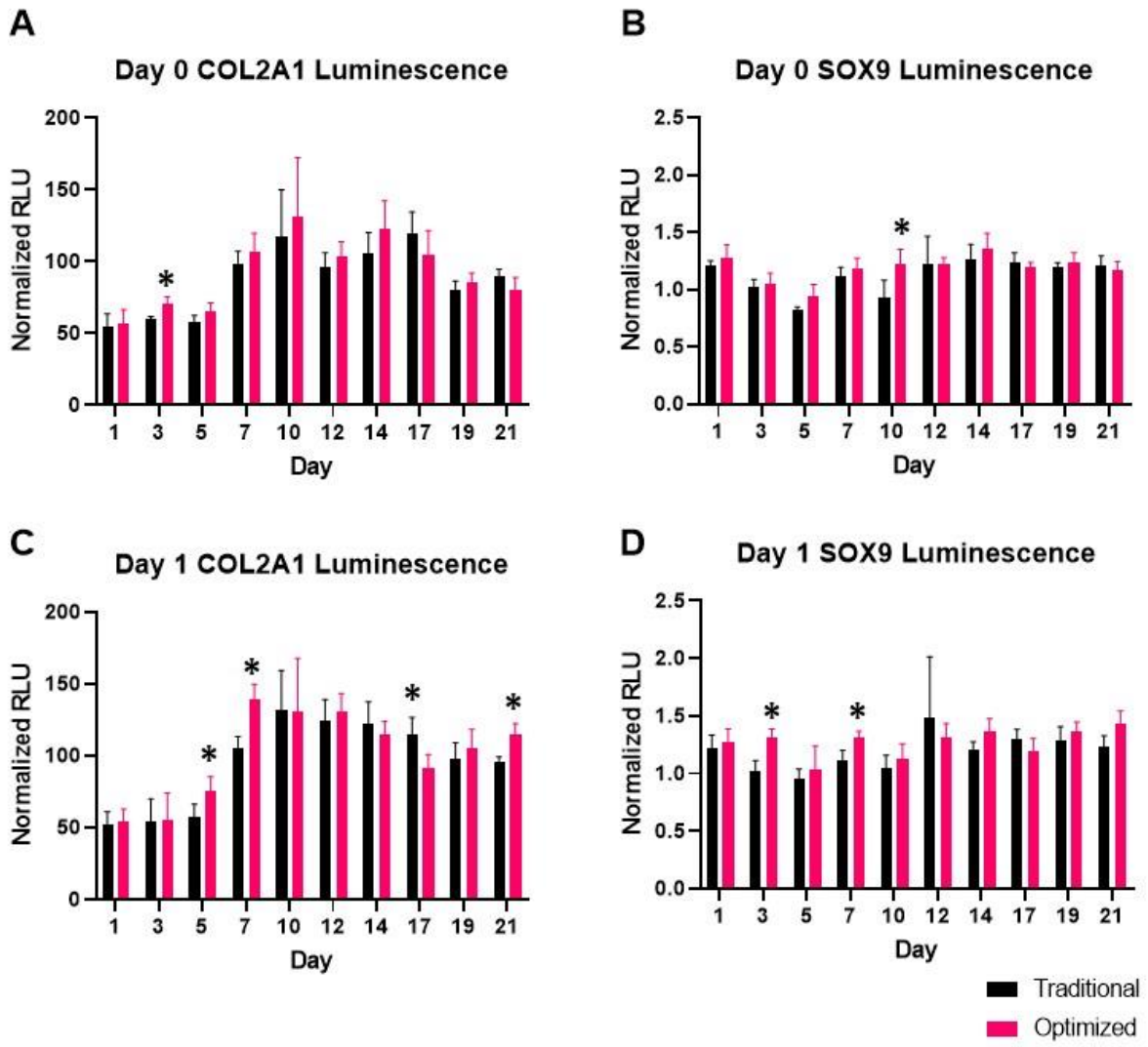

Figure 20: Luminescence of ATDC5-gLuc Cells in Traditional and Optimized Media
Relative light values of ATDC5-gLuc cells normalized to non-infected. * indicates $p < 0.05$ for multiple t-tests of traditional and optimized media.
A: Day 0 COL2A1. B. Day 0 SOX9. C: Day 1 COL2A1. D: Day 1 SOX9.

Optimized media had a significantly higher luminescence on at least one day for both reporters stimulated with vitamins on both day 0 and day 1 (Figure 20), while only day 17 for the COL2A1 reporter stimulated on day 1 was significantly higher luminescence for traditional media over optimized. While these few days of increased luminescence for optimized media is

not overwhelming evidence in its favor, it indicates a potential improvement above the traditional option which can be further validated with qRT-PCR and histology.

Pellet Size Evaluation

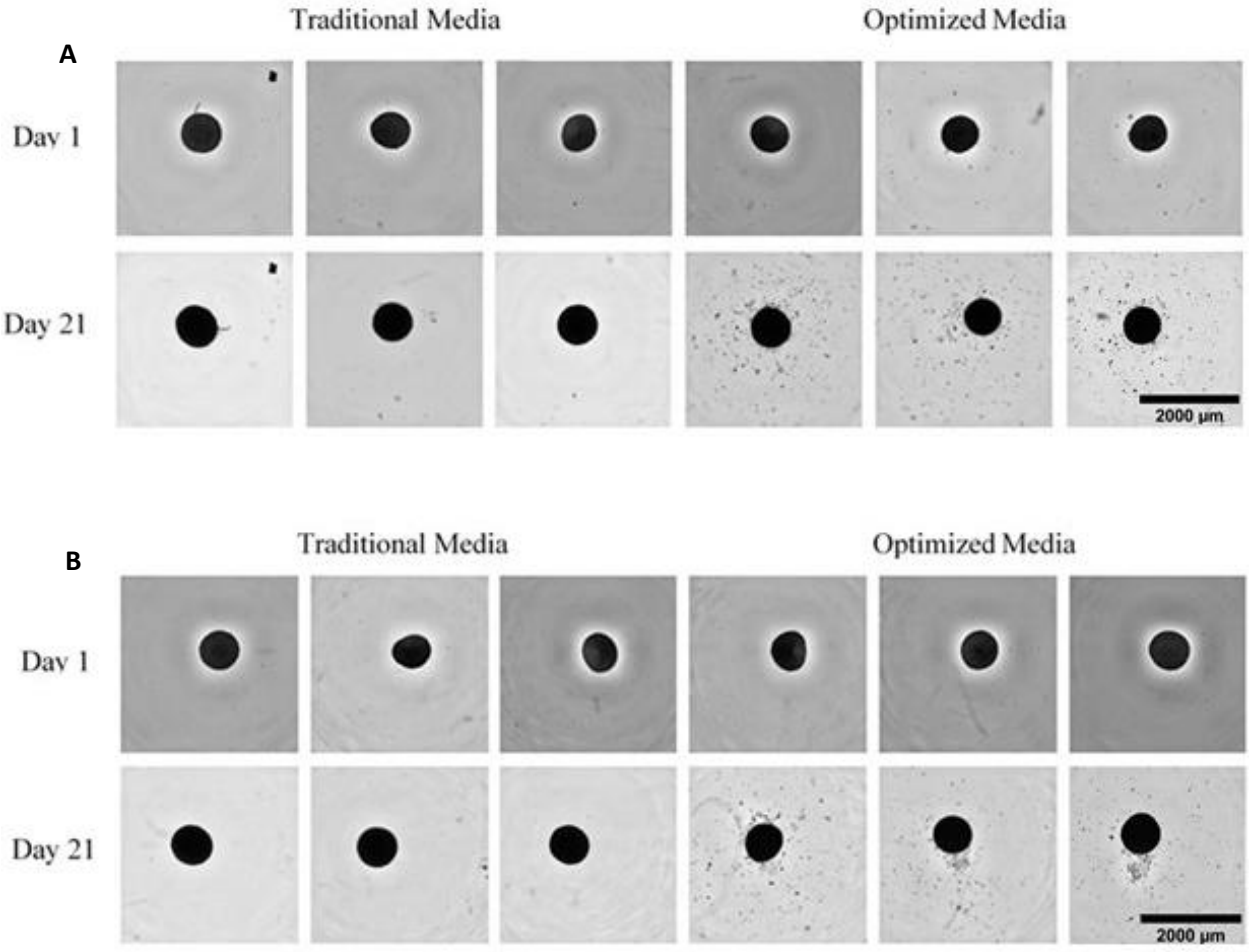

Figure 21: Representative images of Day 0 and Day 1 vitamin pellets
A: Day 0 Pellets B: Day 1 Pellets
From left to right, Traditional (SOX9 reporter, COL2A1 reporter, ATDC5 control) and Optimized (SOX9 reporter, COL2A1 reporter, ATDC5 control). Scale same for each photo.

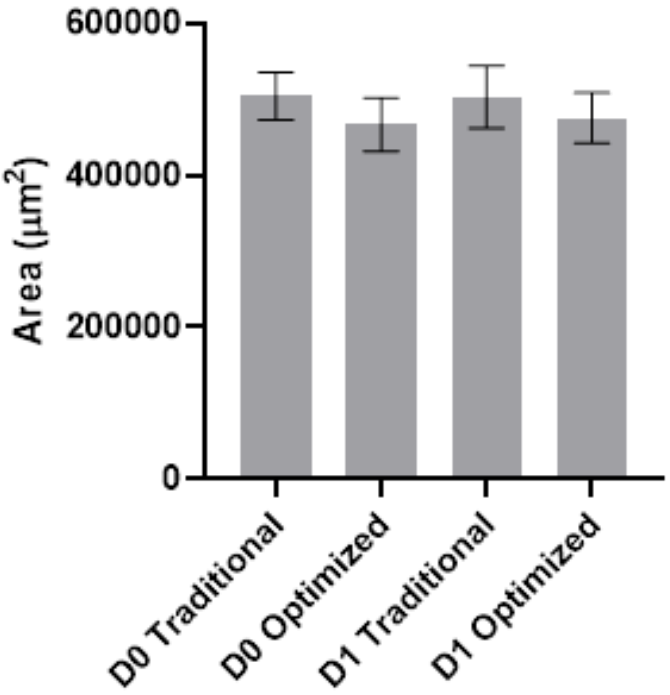

Figure 22: Pellet Size on Day 21
Area of all three pellet types for each of the four growth conditions.

By day 21, there was no significant difference in pellet size between day 0 and day 1 for either traditional or optimized media (Figure 22). However, the pellets grown in traditional media from day 0 were statistically significantly larger than those grown in optimized media by day 21. This is contrary to luminescence signals indicating that type II collagen and SOX9 expression was higher for some days during growth in optimized media. As the Optimized media was adjusted for promotion of type II collagen, it is possible that it is not an ideal media for other ECM proteins such as aggrecan and other proteoglycans, leading to overall smaller pellets despite an increase in type II collagen production.

Additionally, cells grown in optimized media formed small colonies besides the main pellet (Figure 21 A & B) which were not included in the size evaluations. These smaller colonies reveal an interesting effect of vitamin addition on pellet contraction and formation and are more prominent for pellets which were exposed to vitamins in the first 24 hours of contraction (day 0).

qRT-PCR Analysis

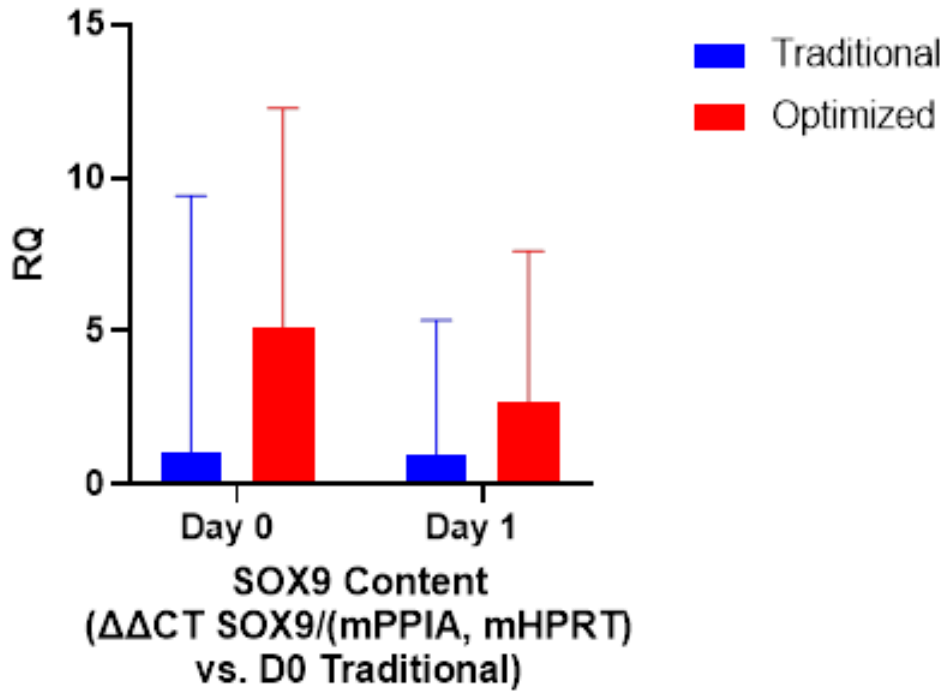

Figure 23: SOX9 Expression for Traditional and Optimized Media
Relative Quantification of SOX9 content compared to D0 traditional media.

While luminescence data indicated that Day 1 addition of media resulted in significantly higher luminescence than for Day 0, including on the last day of sampling, Day 0 addition showed higher RQ for SOX9 with qRT-PCR (Figure 23). Additionally, Optimized media had higher SOX9 expression than Traditional. However, as with the previous qRT-PCR data, pellets result in poor yield and quality mRNA upon lysis, leading to very large error ranges for qRT-PCR. In order to determine if there is an actual discrepancy between the luminescence and qRT-PCR data, improved mRNA yield through additional pellets may be necessary.

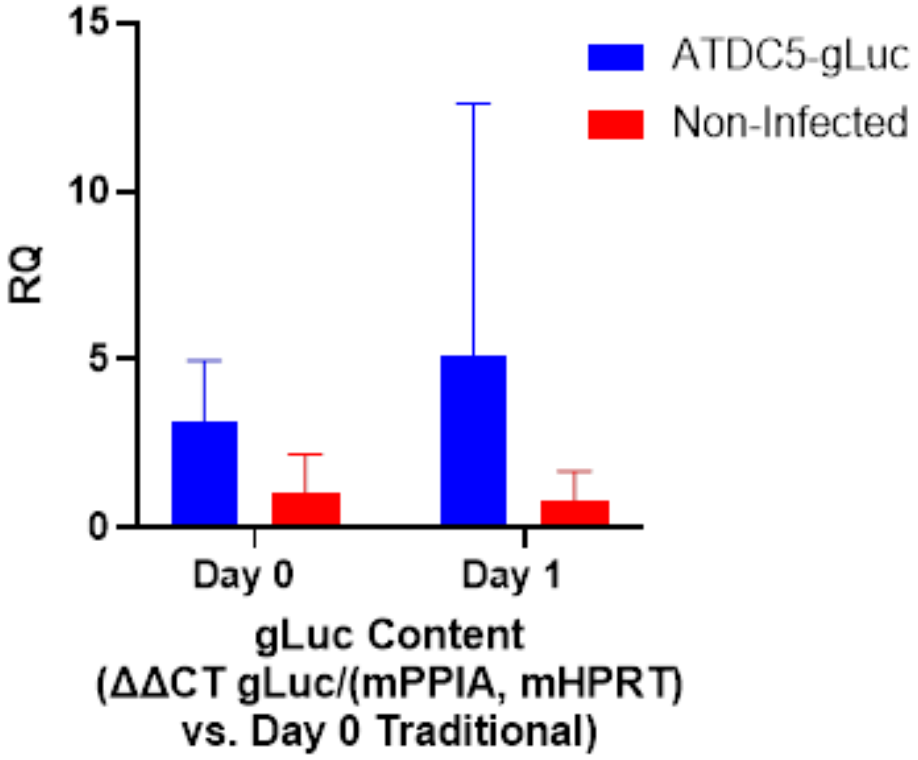

Figure 24: gLuc Expression for ATDC5-gLuc and Non-infected Cells
Relative Quantification of gLuc content compared to D0 traditional media.

An evaluation of gLuc for TGF-β1 dose response pellets for ATDC5-gLuc and non-infected cells gave an amplification curve where only infected cells crossed the threshold value. However, for the growth media experiment, non-infected cell sample did cross the cycle threshold, albeit much later. This is concerning, as non-infected cells should not be expressing any gLuc. In part, the apparent expression of gLuc by non-infected cells may be due to a lower automatic cycle threshold being set by QuantStudio to accommodate the lower gLuc expression for the growth media experiments than TGF-β1. This lower threshold may not prevent primer-dimer formation and off-target amplification from registering as low level gLuc expression.

Histology

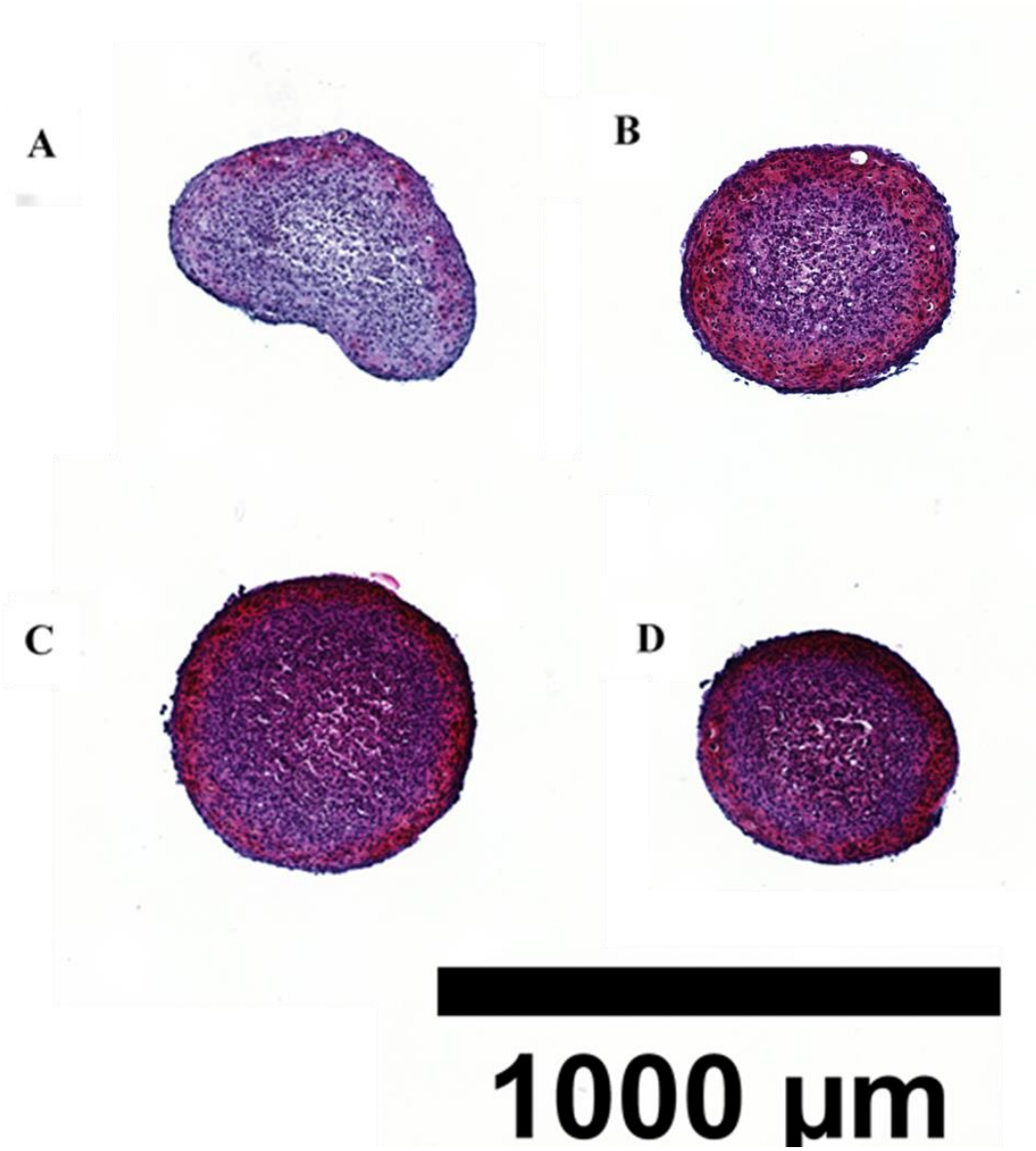

Figure 25: Day 0 vs Day 1 Traditional and Optimized Media Histology
A: Traditional Media, Day 0. B: Optimized Media, Day 0. C: Traditional Media, Day 1. D: Optimized Media, Day 1.

Histology did not reveal any clear differences in proteoglycan content between Day 0 and Day 1 optimized media, nor between Day 1 Traditional and Optimized media (Figure 25). Day 0 Traditional media resulted in a pellet with different shape and staining than the rest. However, this is likely just a difference in pellet orientation during embedding. While the pellets appear spherical, they are actually cup shaped. The sections with a spherical shape were sectioned from the bottom up, while the kidney shaped section is a side view. Given this difference in orientation, it is difficult to attribute the difference any difference in staining to media conditions. The side view reveals a potential difference in proteoglycan expression throughout the pellet, as in Figure 25A, the most intense staining area occurs along the edge of the pellet on what would be the surface contacting the bottom of the wells. When sectioned from the bottom up, this intense band along the edge would manifest as a ring of strong staining around the outside of the pellet (Figures 25 B-D).

Infection rates and viral titers were low resulting in poor initial infection of cells, but despite poor transfection the luminescent signal was seen to be non-transient and infection did not result in obvious metabolic changes. A potential temporal shift in TGF-β1 stimulated chondrogenesis was seen at lower doses, highlighting the need for a non-destructive reporter, and a difference in SOX9 and COL2A1 expression with media type and vitamin addition time was observed. Both of these topics are prospective avenues of further investigation using an improved promotor-driven secreted luciferase reporter system. Reporter cell improvements will include increasing infection rates of cell through generation of additional lentivirus and reinfection, as well as the development of an improved assay buffer with increased buffering capability.

REFERENCES

1. Hunter, D.J. and S. Bierma-Zeinstra, *Osteoarthritis.* Lancet, 2019. **393**(10182): p. 1745-1759.
2. Disease, G.B.D., I. Injury, and C. Prevalence, *Global, regional, and national incidence, prevalence, and years lived with disability for 354 diseases and injuries for 195 countries and territories, 1990-2017: a systematic analysis for the Global Burden of Disease Study 2017.* Lancet, 2018. **392**(10159): p. 1789-1858.
3. Murphy, L.B., et al., *Medical Expenditures and Earnings Losses Among US Adults With Arthritis in 2013.* Arthritis Care Res (Hoboken), 2018. **70**(6): p. 869-876.
4. Gore, M., et al., *Use and costs of prescription medications and alternative treatments in patients with osteoarthritis and chronic low back pain in community-based settings.* Pain Pract, 2012. **12**(7): p. 550-60.
5. Bannuru, R.R., et al., *OARSI guidelines for the non-surgical management of knee, hip, and polyarticular osteoarthritis.* Osteoarthritis Cartilage, 2019. **27**(11): p. 1578-1589.
6. Varacallo, M., T.D. Luo, and N.A. Johanson, *Total Knee Arthroplasty (TKA) Techniques*, in *StatPearls*. 2020: Treasure Island (FL).
7. Centers for Disease, C. and Prevention, *Prevalence and most common causes of disability among adults--United States, 2005.* MMWR Morb Mortal Wkly Rep, 2009. **58**(16): p. 421-6.
8. Lawrence, R.C., et al., *Estimates of the prevalence of arthritis and other rheumatic conditions in the United States. Part II.* Arthritis Rheum, 2008. **58**(1): p. 26-35.

9. Losina, E., et al., *Lifetime medical costs of knee osteoarthritis management in the United States: impact of extending indications for total knee arthroplasty.* Arthritis Care Res (Hoboken), 2015. **67**(2): p. 203-15.

10. Lo, J., L. Chan, and S. Flynn, *A Systematic Review of the Incidence, Prevalence, Costs, and Activity/Work Limitations of Amputation, Osteoarthritis, Rheumatoid Arthritis, Back Pain, Multiple Sclerosis, Spinal Cord Injury, Stroke, and Traumatic Brain Injury in the United States: A 2019 Update.* Arch Phys Med Rehabil, 2020.

11. Brittberg, M., et al., *Treatment of deep cartilage defects in the knee with autologous chondrocyte transplantation.* N Engl J Med, 1994. **331**(14): p. 889-95.

12. Gikas, P.D., et al., *An overview of autologous chondrocyte implantation.* J Bone Joint Surg Br, 2009. **91**(8): p. 997-1006.

13. Micheli, L.J., et al., *Autologous chondrocyte implantation of the knee: multicenter experience and minimum 3-year follow-up.* Clin J Sport Med, 2001. **11**(4): p. 223-8.

14. Correa, D. and S.A. Lietman, *Articular cartilage repair: Current needs, methods and research directions.* Semin Cell Dev Biol, 2017. **62**: p. 67-77.

15. Temenoff, J.S. and A.G. Mikos, *Review: tissue engineering for regeneration of articular cartilage.* Biomaterials, 2000. **21**(5): p. 431-40.

16. Huang, B.J., J.C. Hu, and K.A. Athanasiou, *Cell-based tissue engineering strategies used in the clinical repair of articular cartilage.* Biomaterials, 2016. **98**: p. 1-22.

17. Zhang, L., J. Hu, and K.A. Athanasiou, *The role of tissue engineering in articular cartilage repair and regeneration.* Crit Rev Biomed Eng, 2009. **37**(1-2): p. 1-57.

18. Minas, T., et al., *The John Insall Award: A minimum 10-year outcome study of autologous chondrocyte implantation.* Clin Orthop Relat Res, 2014. **472**(1): p. 41-51.

19. de Crombrugghe, B., et al., *Transcriptional mechanisms of chondrocyte differentiation.* Matrix Biol, 2000. **19**(5): p. 389-94.

20. Tew, S.R., et al., *SOX9 transduction of a human chondrocytic cell line identifies novel genes regulated in primary human chondrocytes and in osteoarthritis.* Arthritis Res Ther, 2007. **9**(5): p. R107.

21. Bi, W., et al., *Sox9 is required for cartilage formation.* Nat Genet, 1999. **22**(1): p. 85-9.

22. Pan, Q., et al., *Sox9, a key transcription factor of bone morphogenetic protein-2-induced chondrogenesis, is activated through BMP pathway and a CCAAT box in the proximal promoter.* J Cell Physiol, 2008. **217**(1): p. 228-41.

23. Benya, P.D. and J.D. Shaffer, *Dedifferentiated chondrocytes reexpress the differentiated collagen phenotype when cultured in agarose gels.* Cell, 1982. **30**(1): p. 215-24.

24. Marlovits, S., et al., *Changes in the ratio of type-I and type-II collagen expression during monolayer culture of human chondrocytes.* J Bone Joint Surg Br, 2004. **86**(2): p. 286-95.

25. Schnabel, M., et al., *Dedifferentiation-associated changes in morphology and gene expression in primary human articular chondrocytes in cell culture.* Osteoarthritis Cartilage, 2002. **10**(1): p. 62-70.

26. Kock, L., C.C. van Donkelaar, and K. Ito, *Tissue engineering of functional articular cartilage: the current status.* Cell Tissue Res, 2012. **347**(3): p. 613-27.

27. Whitney, G.A., et al., *Scaffold-free cartilage subjected to frictional shear stress demonstrates damage by cracking and surface peeling.* J Tissue Eng Regen Med, 2017. **11**(2): p. 412-424.

28. Kean, T.J., et al., *Disparate response of articular- and auricular-derived chondrocytes to oxygen tension.* Connect Tissue Res, 2016. **57**(4): p. 319-33.

29. Kean, T.J. and J.E. Dennis, *Synoviocyte Derived-Extracellular Matrix Enhances Human Articular Chondrocyte Proliferation and Maintains Re-Differentiation Capacity at Both Low and Atmospheric Oxygen Tensions.* PLoS One, 2015. **10**(6): p. e0129961.

30. Correa, D., R.A. Somoza, and A.I. Caplan, *Nondestructive/Noninvasive Imaging Evaluation of Cellular Differentiation Progression During In Vitro Mesenchymal Stem Cell-Derived Chondrogenesis.* Tissue Eng Part A, 2018. **24**(7-8): p. 662-671.

31. Archer, C.W. and P. Francis-West, *The chondrocyte.* Int J Biochem Cell Biol, 2003. **35**(4): p. 401-4.

32. Sophia Fox, A.J., A. Bedi, and S.A. Rodeo, *The basic science of articular cartilage: structure, composition, and function.* Sports Health, 2009. **1**(6): p. 461-8.

33. Liu, C.F. and V. Lefebvre, *The transcription factors SOX9 and SOX5/SOX6 cooperate genome-wide through super-enhancers to drive chondrogenesis.* Nucleic Acids Res, 2015. **43**(17): p. 8183-203.

34. Atsumi, T., et al., *A chondrogenic cell line derived from a differentiating culture of AT805 teratocarcinoma cells.* Cell Differ Dev, 1990. **30**(2): p. 109-16.

35. Yao, Y. and Y. Wang, *ATDC5: an excellent in vitro model cell line for skeletal development.* J Cell Biochem, 2013. **114**(6): p. 1223-9.

36. Shukunami, C., et al., *Sequential progression of the differentiation program by bone morphogenetic protein-2 in chondrogenic cell line ATDC5.* Exp Cell Res, 1998. **241**(1): p. 1-11.

37. Oh, C.D., et al., *SOX9 regulates multiple genes in chondrocytes, including genes encoding ECM proteins, ECM modification enzymes, receptors, and transporters.* PLoS One, 2014. **9**(9): p. e107577.

38. Tsang, K.Y., D. Chan, and K.S. Cheah, *Fate of growth plate hypertrophic chondrocytes: death or lineage extension?* Dev Growth Differ, 2015. **57**(2): p. 179-92.

39. Akkiraju, H. and A. Nohe, *Role of Chondrocytes in Cartilage Formation, Progression of Osteoarthritis and Cartilage Regeneration.* J Dev Biol, 2015. **3**(4): p. 177-192.

40. Wong, C.H., K.W. Siah, and A.W. Lo, *Estimation of clinical trial success rates and related parameters.* Biostatistics, 2019. **20**(2): p. 273-286.

41. Wouters, O.J., M. McKee, and J. Luyten, *Estimated Research and Development Investment Needed to Bring a New Medicine to Market, 2009-2018.* JAMA, 2020. **323**(9): p. 844-853.

42. Maguire, C.A., et al., *Gaussia luciferase variant for high-throughput functional screening applications.* Anal Chem, 2009. **81**(16): p. 7102-6.

43. Durand, S. and A. Cimarelli, *The inside out of lentiviral vectors.* Viruses, 2011. **3**(2): p. 132-59.

44. Dennis, J.E., T. Splawn, and T.J. Kean, *High-Throughput, Temporal and Dose Dependent, Effect of Vitamins and Minerals on Chondrogenesis.* Front Cell Dev Biol, 2020. **8**: p. 92.

45. Dull, T., et al., *A third-generation lentivirus vector with a conditional packaging system.* J Virol, 1998. **72**(11): p. 8463-71.

46. Jiang, W., et al., *An optimized method for high-titer lentivirus preparations without ultracentrifugation.* Sci Rep, 2015. **5**: p. 13875.

47. Haddock, S.H.D., C.M. McDougall, and J.F. Case. *The Bioluminescence Web Page*. 1997 2020 [cited 2020; Available from: https://biolum.eemb.ucsb.edu/.